

NAVIGATING GALILEO IN THE JOVIAN SYSTEM

P.G. Antreasian, T.P. McElrath, R.J. Haw, G.D. Lewis
Jet Propulsion Laboratory, California Institute of Technology, Pasadena, California 91109

Abstract

The Galileo spacecraft's navigation results for the first eleven Jupiter satellite encounters are described. The achieved performance is compared against predicted accuracies. The average target miss in the satellite's B-plane coordinate frame (compared against post-encounter reconstruction) was 0.9σ in B•R, 0.6σ in B•T, and 1.6σ in encounter time, with the largest single error being 3.4σ in B•R. This performance preserved sufficient on-board propellant to enable a follow-on mission of up to four years.

Introduction

The Galileo spacecraft, functioning and in orbit around Jupiter at the time of this writing, has completed its primary mission. Jupiter, its magnetosphere, and the four Galilean moons (Io, Europa, Ganymede, and Callisto) have all been closely observed. This paper will describe the navigation results of Galileo's first dozen orbits around Jupiter (with an emphasis on orbit determination), and compare these results with *a priori* goals and error analyses. The latest estimates of Jovian satellite ephemerides and gravity are also presented. Background material on Galileo's mission is documented in the literature.¹⁻⁹

Navigation Strategies

The Spacecraft Trajectory

The Galileo spacecraft completed twelve orbits around Jupiter through 1997, with eleven satellite encounters at altitudes between 200 and 3100 km. Each orbit was characterized by a close flyby of either Europa, Ganymede, or Callisto and is designated by a letter and a number indicating the satellite and orbit. For example, G2 indicates that in its second orbit, Galileo passed closest to Ganymede.

Galileo's trajectory was designed with gravity-assists at each encounter in order to re-direct the spacecraft toward subsequent encounters along a ballistic (or nearly ballistic) path.⁹ We report on the navigation outcome at these encounters. Table 1 lists the dates of the encounters and the achieved altitudes and latitudes. Also important to the mission for science opportunities were the so-called non-targeted satellite encounters with altitudes from 20,000 to 80,000 km. The non-targeted satellites are denoted in Table 1 with an 'A' following the encounter number. A trajectory pole view of Galileo's first twelve orbits around Jupiter is shown in Figure 1.

Orbit Trim Maneuvers

Trajectory control in orbit was provided with periodic thrusting events, or orbit trim maneuvers (OTMs). Three orbit trim maneuvers were planned per orbit (more if needed). Maneuvers at apoJove were often explicitly designed to change the spacecraft's orbital characteristics in order to meet our objectives (such as Io occultations). Pre-encounter and post-encounter OTMs were designed to remove navigation errors, steering the spacecraft back to the correct path. These maneuvers occurred approximately three days before and after each satellite encounter. The pre-encounter maneuver was first designed during the initial approach

to an encounter and was often updated one week later (still before the encounter) with the latest tracking data. This new data led to a modified maneuver design, denoted as a “tweak”, which reproduced the intended trajectory more accurately than the initial design. After each flyby the future trajectory was reoptimized by adjusting the targets at the remaining flybys (using propellant usage as the cost function).

Table 1 Satellite Encounter Dates, Flyby Altitudes, and Latitudes

Enc	OWLT‡ (min)	Inbound/ Outbound	Date‡ (SCET-UTC) ± (s)	Altitude (km)	Latitude† (deg)	Solution Designation
G1	35	In	27-Jun-96 06:29:06.70 ± 0.005	835.22 ± 0.03	30.392 ± 0.002	OD123
G2	39	In	06-Sep-96 18:59:33.88 ± 0.02	260.65 ± 0.50	79.282 ± N.A.	OD135
C3	46	In	04-Nov-96 13:34:28.00 ± 0.005	1135.96 ± 0.04	13.192 ± 0.002	OD142
E3A	46	Out	06-Nov-96 18:49:51.31 ± 0.07	34,786.51 ± 1.45	0.701 ± 0.026	OD143
E4	50	Out	19-Dec-96 06:52:57.70 ± 0.01	692.05 ± 0.10	-1.670 ± 0.036	OD151
E5A	51	Out	20-Jan-97 01:08:37.00 ± 0.31	26,667.83 ± 0.29	-0.821 ± 0.007	OD155
E6	50	In	20-Feb-97 17:06:10.20 ± 0.01	586.33 ± 0.07	-17.020 ± 0.004	OD159
E7A	46	In	04-Apr-97 05:58:47.56 ± 0.05	23,487.08 ± 0.31	2.137 ± 0.005	OD166
G7	46	Out	05-Apr-97 07:09:58.10 ± 0.005	3101.85 ± 0.04	55.797 ± <0.0005	OD167
C8A	42	In	06-May-97 12:10:27.75 ± 0.67	33,060.56 ± 0.46	-42.001 ± 0.001	OD171
G8	42	In	07-May-97 15:56:09.55 ± 0.005	1603.24 ± 0.03	28.271 ± 0.001	OD172
C9	36	In	25-Jun-97 13:47:49.95 ± 0.005	418.09 ± 0.03	1.963 ± 0.012	OD181
G9A	36	In	26-Jun-97 17:19:34.31 ± 0.005	79,741.06 ± 0.18	-0.018 ± 0.011	OD180
C10	35	In	17-Sep-97 00:18:54.78 ± <0.001	535.31 ± 0.01	4.598 ± 0.004	OD187
E11	41	In	06-Nov-97 20:31:44.21 ± 0.003	2043.26 ± 0.03	25.730 ± 0.001	OD192
G12A	47	In	15-Dec-97 09:58:09.34 ± 0.002	14,402.54 ± 0.03	-5.817 ± 0.001	OD197
E12	47	Out	16-Dec-97 12:03:19.86 ± 0.001	200.99 ± 0.15	-8.680 ± 0.003	OD197

† Satellite True Equator of Date (STED)

‡ To compute Earth Received Time (ERT), add one way light time (OWLT) to Spacecraft Event Time (SCET)

Spacecraft Tracking Systems

Galileo is monitored with two-way coherent S-Band radio transmissions via the NASA/JPL Deep Space Network’s (DSN) 70 meter antennas in Goldstone (California), Canberra (Australia) and Madrid (Spain). Navigation data consists of Doppler measurements extracted from the radio signal as well as optical navigation (OPNAV) data acquired with the on-board CCD spacecraft camera. OPNAVs compliment the Doppler, providing an orthogonal component to the data set. Doppler tracking, however, was impacted appreciably when the high gain antenna failed to open after launch -- lowering the gain over the remaining low gain antenna by about 40 dB.⁷ The lower gain also limited the number of OPNAV images returned per orbit because of the reduced data return capability of the telecommunication system. This limitation was partly overcome by placing software onboard Galileo to compress and edit images before downlinking to Earth.

Each OPNAV image consisted of one (or more) Galilean satellites shuttered against a reference stellar background. The camera’s field-of-view is 10 microradians per pixel, with an accuracy of 0.33 pixel (1-σ). Assuming astrometric knowledge of the star is reliable, then star-relative satellite position knowledge of 15

km were obtainable. This provided valuable information on mean longitude and out-of-plane motion, two parameters essentially invisible to radiometric data. Dynamical knowledge could then be inferred for Io, Europa, and Ganymede from their Laplacian resonance and to a lesser degree, Callisto.

As an illustration of this data type, a schematic representation of a sequence of OPNAV's from the spacecraft's approach to the G7 encounter, as viewed through the spacecraft camera, is reproduced in Figure 2. The frame coordinates are pixels, representing the 800 x 800 pixel spacecraft camera. The sunlit crescent of Ganymede (and sometimes Io, serendipitously) is framed in these fields-of-view, along with a reference star. (Stars, marked with a "+", are not identified in the figure; the number adjacent to the star indicates its visual magnitude). Listed beneath each frame from left to right are an identification number, the range from Galileo to Ganymede, and the cone angle (angle between the Earth-pointed spacecraft axis and the camera boresight axis). Eight to thirty-three OPNAV's per orbit were returned, yielding a total of one hundred thirty-eight for the mission (OPNAV's were not acquired after G7). Figure 3 illustrates a trajectory-pole view geometry of Galileo's OPNAV shutterings.

Satellite Ephemeris (Integrated versus Theory)

Pre-launch tour navigation studies were founded on analytical satellite ephemerides, which limited satellite knowledge to ~10 km.¹⁰ Comparisons later made between the analytical ephemeris and integrated ephemerides showed large secular and periodic downtrack differences, and observational data of Jupiter's moons strongly supported the integrated ephemeris.² Thus in 1995 the Galileo Navigation team decided in favor of an integrated satellite ephemeris for tour navigation.

The initial integrated satellite ephemeris, labelled JUP076, was based on spacecraft encounter data and ground-based observations to 1994. In May 1996 a new baseline integrated ephemeris and *a priori* covariance (used to constrain satellite states), labelled JUP088, were released for tour operations.

Orbit Determination (OD)

Controlling a spacecraft trajectory constrained by finite propellant reserves is an optimization problem -- the first step of which is to accurately determine the spacecraft state. The spacecraft's trajectory is integrated from the estimated initial state and each satellite's orbit iteratively improved. Our state estimation procedure follows well-established techniques employing a batch sequential pseudo-epoch-state least-squares filter. Table A-1 in the appendix lists parameters and *a priori* values used in the filter.

We wish to make a point of discussing the solar radiation pressure model. In general our model was stable and consistent, and we saw no evidence for unmodelled gravitational forces.¹¹ During the Jupiter approach phase however (before the tour), we discovered that spacecraft thermal emissions emanating from the sub-solar direction (especially from the radioisotope thermal generators) were of similar magnitude to the solar radiation pressure -- in effect decreasing the solar radiation pressure. This contribution was consistently determined to be 0.4 nm/s² (cf. solar radiation pressure determination of 3.3 nm/s² at 5.2 AU). During the tour, to reduce the number of estimated parameters, the spacecraft's thermal emission was combined into the

solar pressure model (effectively by lowering the reflectivity coefficients).

With the above modeling methods we were able to precisely determine spacecraft state with respect to the encounter body at the time of each flyby. Therefore as a performance metric, we compare each pre-encounter solution with its post-encounter solution, as well as with the target. (The post-encounter solution is also labelled the reconstruction.) Results from the first eleven encounters are presented below.

Navigation Results

The insertion burn placing Galileo into orbit around Jupiter occurred on December 8, 1995.⁶ Between that time and June, 1996 four additional maneuvers occurred, including a maneuver on March 14 of magnitude 376 m/s to raise the perijove of Galileo and send the spacecraft on to Ganymede, the first encounter of the tour. The results described herein begin June 1, twenty-six days before the Ganymede encounter. The following sections summarize each encounter briefly. More details can be found in Ref. 2.

G1 Approach & Encounter (Refer to Figure 4 and Table 2)

The first G1 targetting maneuver to correct the inbound trajectory, OTM-5, was designed from the solution labelled **OD115** using a radiometric (Doppler) data arc from December 8, 1995 to June 5, 1996. **OD115** also contained two distant OPNAV images of Ganymede. The residual scatter of these data were 0.006 mm/s rms for the Doppler and 0.17 pixel rms for the optical data, indicating a good match between the data and the trajectory model. **OD115** determined that the spacecraft would pass within 907 km and 131 seconds of the target. Prior to **OD115** the 1- σ Ganymede ephemeris uncertainties, taken from the JUP088 covariance, were 9.7 km, 41.5 km, 71.3 respectively in the radial (R), downtrack or transverse (T), and out-of-plane or normal (N) directions. By incorporating the two OPNAVs, the Ganymede ephemeris shifted -4.5 ± 9.6 km in the radial, -32.6 ± 40.9 km in the downtrack, and 5.1 ± 71.3 km in the out-of-plane directions -- significant movement, but still sub-sigma (note that there was no improvement in the uncertainties). OTM-5 thrusted on June 12, 1996 (fifteen days before G1) with a ΔV of 0.53 m/s to redirect Galileo to the target. One more maneuver at three days before the encounter further refined the G1 targetting. A total of thirty-three OPNAVs were shuttered with a success rate of 76%.

The post-encounter reconstruction **OD123** determined that the error in the trajectory prediction was less than 1- σ of predicted uncertainties, with respect to the latest pre-encounter solution **OD118**, missing the target by 0.5 σ in both the B•R and B•T directions (-8.7 km, -15 km), but arriving late by 1.6 σ (2.7sec). Ganymede shifted -16 km (2 σ) in the radial, -22 km (0.7 σ) in the downtrack and -6 km (0.4 σ) in the out-of-plane directions.

Table 2 Orbit Determination Solutions Supporting the G1 Encounter on 27 June 1996

OD	OTM	DCO	B•R	B•T	TCA	σ SMA	σ SMI	Θ
----	-----	-----	-----	-----	-----	--------------	--------------	----------

		(km)	(km)	(SCET UTC)	(km)	(km)	(deg)
Target		-1835.7	3157.9	06:29:04.0			
OD115	5 G1-22d	-1717.0 ± 73.2	4056.9 ± 48.0	06:26:53.3 ± 5.14	73.3	47.8	86.0
OD117	6 G1-11d	-1837.9 ± 23.4	3189.3 ± 40.9	06:29:00.5 ± 4.03	41.0	23.3	175.7
OD118	6t G1-3.5d	-1860.4 ± 16.2	3236.4 ± 30.5	06:28:55.0 ± 1.65	30.7	15.9	172.9
OD123	7 G1+10h	-1844.4 ± 0.1	3142.9 ± 0.1	06:29:06.7 ± <0.05	0.1	<0.05	53.3
OD128	8 G1+Apo	-1844.5 ± 0.3	3142.6 ± 0.2	06:29:06.7 ± <0.05	0.4	0.1	66.0

G2 Approach & Encounter (Refer to Figure 5 and Table 3)

The G1 post-encounter solution **OD123** determined that the second orbit's period was short of the design value by approximately 63 minutes. OTM-7 corrected this energy error, thrusting on 30 June 1996 with a ΔV of $0.59 \text{ m/s} \pm 0.01\%$. The G2 *reference*¹ aimpoint was selected after the design of OTM-7, fixing the flyby of Ganymede on 6 September 1996 at 18:59.0 UTC at an altitude of 262 km. To reach G2, an apojove maneuver was required to adjust the inclination of the spacecraft's orbit. OTM-8 was implemented on 5 August 1996 with a ΔV of $4.60 \text{ m/s} \pm 0.14\%$. OTM-9 further refined the in-bound trajectory while the final G2 trajectory correction update opportunity, the tweak of OTM-10, was judged to be unnecessary and was cancelled.

To preserve the Ganymede ephemeris knowledge acquired from the first encounter, an updated JUP088 covariance derived from the G1 encounter data was incorporated in solutions **OD130 - OD135**.

The first two OPNAV's of Ganymede-2 were received August 10, 1996. These data fit the trajectory model well, yielding a residual scatter of 0.02 pixels rms, in agreement with the G1 satellite ephemeris computed from **OD128**. In total, nine OPNAV's (seven of Ganymede and two of Europa) were included in the final pre-encounter solution **OD132**. The Ganymede OPNAV's exhibited small residuals, but the Europa images displayed residuals on the order of 0.5 pixels (indicating a poor fit to the Europa data and a possible inconsistency with Europa's orbit).

The *a posteriori* G2 reconstruction fell within the $1\text{-}\sigma$ B-plane dispersions of OTM-10 and 10t, but arrived earlier by greater than $1\text{-}\sigma$.

Table 3: Orbit Determination Solutions Supporting the G2 Encounter on 9 September 1996

OD	OTM	DCO	B•R (km)	B•T (km)	TCA (SCET UTC)	σ SMA (km)	σ SMI (km)	Θ (deg)
----	-----	-----	-------------	-------------	-------------------	----------------------	----------------------	-------------------

¹The tour was reoptimized after every encounter. A new *reference* trajectory was designed using a post-encounter OD solution to update the orbiter trajectory and satellite ephemeris using several hours to a few days of tracking data after each encounter, but usually before the post-encounter OTM design. Since much of the sequence work (orbit planning) was performed several months in advance, tour reoptimization was constrained to only allow changes in subsequent encounter targets of up to ± 50 km in the latitude and cross-latitude (altitude) directions and to remain within ± 3 minutes on even minutes. Trajectory design constraints consisted of these maximum offsets from the reference aimpoints and the Io occultations on orbits E6 and C9. Given these constraints, science observations could be shifted as a block and slightly retargeted in the sequence design.

Target			-3019.1		535.1		18:59:39.0			
OD128	8	G2-42.5d	300.4 ± 1.0		21214.7 ± 19.6		18:08:10.0 ± 2.5	19.6	0.7	2.2
OD130	9	G2-18.5d	-3003.6 ± 6.8		629.8 ± 21.5		18:59:25.3 ± 2.9	21.6	6.5	5.7
OD131	10	G2-9d	-3016.7 ± 5.7		538.0 ± 14.4		18:59:34.5 ± 1.7	14.4	5.6	3.0
OD132	10t	G2-3d	-3016.4 ± 5.3		537.9 ± 6.9		18:59:34.3 ± 0.3	6.9	5.3	8.2
OD135	11	G2+11h	-3015.1 ± 0.5		548.4 ± 0.4		18:59:33.9 ± <0.05	0.5	0.4	95.0
OD137	12	G2+Apo	-3015.8 ± 0.4		548.3 ± 0.1		18:59:33.9 ± <0.05	0.4	<0.05	109.0

C3 Approach & Encounter (Refer to Figure 6 and Table 4)

The period of orbit three, determined by **OD135**, was short of the design value by approximately 6.5 hours. To increase the period, OTM-11 was executed on September 9, 1996 with a ΔV of 4.8 m/s. For the C3 pre-encounter maneuver, OTM-13, seventeen of twenty-six OPNAVs were successful. The final trajectory correction update opportunity, the tweak of OTM-13, was judged to be unnecessary and was cancelled.

The reconstruction of the C3 encounter (**OD142**) concluded that Galileo flew within both the 1- σ dispersions of **OD139** and the OTM-12 delivery. The difference between the reconstructed flyby of **OD142** and pre-encounter solution, **OD139** was 0.2 σ in both TCA and B•R, and 0.6 σ for B•T. The Callisto ephemeris moved -20 km from the **OD139** solution in downtrack and -32 km in the out-of-plane direction.

Table 4: Orbit Determination Solutions Supporting the C3 Encounter on 4 November 1996

OD	OTM	DCO	B•R (km)	B•T (km)	TCA (SCET UTC)	σ SMA (km)	σ SMI (km)	Θ (deg)
Target			-867.8	3534.9	13:34:27.0			
OD135	11	G2+11h	-2243.7 ± 22.5	190650.0 ± 399.1	08:18:24.7 ± 39.4	399.1	22.5	0.2
OD137	12	C3-38d	-837.1 ± 26.3	3929.4 ± 44.9	13:35:50.4 ± 2.8	44.9	26.3	178.3
OD138	13	C3-12d	-863.0 ± 20.5	3527.7 ± 38.8	13:34:26.9 ± 1.7	38.8	20.5	178.8
OD139	13t	C3-4.5d	-851.4 ± 15.9	3535.7 ± 34.6	13:34:27.4 ± 1.6	34.6	15.9	179.0
OD142	14	C3+1d	-853.8 ± 0.1	3557.4 ± <0.05	13:34:27.7 ± <0.05	0.1	<0.05	84.8
OD145	15	C3+Apo	-853.8 ± 0.1	3557.0 ± <0.05	13:34:27.7 ± <0.05	0.1	<0.05	85.0

E4 Approach & Encounter (Refer to Figure 7 and Table 5)

The post-C3 period (orbit-4), determined by **OD142**, was greater than the required period by 49 minutes. Consequently OTM-14 was designed with a ΔV of 2.3 m/s to remove excess orbital energy. In the E4 B-plane, OTM-14 slid the trajectory-intercept point across Europa's disk, adjusting the trajectory so that Galileo's flyby occurred in front of Europa. At the encounter, Galileo was occulted by Europa, interrupting the signal from one minute before the encounter to eleven minutes afterwards.

Europa's ephemeris, from the reconstruction **OD151**, was found to have shifted 10 km (over 1- σ) in the downtrack direction and 11.2 km (almost 1- σ) in the out-of-plane direction, as compared to the pre-encounter ephemeris **OD148**. Even with this relatively large difference, **OD151** remained within the 1- σ

delivery ellipse of OTM-16 (pre-encounter maneuver). The target was missed by 12 ± 1.5 km in B•R, 6.4 km in B•T and 1 sec in TCA. The large B•R uncertainty in the reconstruction was a result of the equatorial flyby. The OPNAV success rate was 88%.

Table 5: Orbit Determination Solutions Supporting the E4 Encounter on 19 December 1996

OD	OTM	DCO	B•R (km)	B•T (km)	TCA (SCET UTC)	σ SMA (km)	σ SMI (km)	Θ (deg)
Target			46.5	-2367.9	06:52:56.7			
OD142	14	C3+1d	-259.4 \pm 18.6	24418.7 \pm 2142.4	09:05:42.6 \pm 495.4	2142.4	18.5	179.9
OD145	15	E4-30.5d	34.7 \pm 15.9	-1522.3 \pm 12.3	06:58:16.6 \pm 4.0	15.9	12.3	85.5
OD146	16	E4-10d	53.0 \pm 14.5	-2358.9 \pm 6.3	06:53:00.2 \pm 1.9	14.5	6.3	89.1
OD148	16t	E4-5d	54.6 \pm 11.3	-2354.8 \pm 4.7	06:53:01.4 \pm 1.4	11.3	4.7	88.4
OD151	17	E4+19h	58.4 \pm 1.5	-2361.5 \pm 0.1	06:52:57.7 \pm <0.05	1.5	0.1	90.8
OD155	19	E5A+Apo	57.3 \pm 0.5	-2361.5 \pm <0.05	06:52:57.7 \pm <0.05	0.5	<0.05	90.0

E6 Approach & Encounter (Refer to Figure 8 and Table 6)

Four days after the E4 encounter OTM-17 corrected the flyby errors and changed the period of orbit-5 by 31 minutes ($\Delta V = 2$ m/s). The orbit following E4, orbit 5 was a *phasing* orbit, a quiescent orbit designed to avoid important activities during the extant solar conjunction (January 10- 27, 1997). No targeted encounter was planned during this orbit. After a second orbit of Jupiter, upon approach to E6, Europa's state was judged sufficiently well known to cancel the E6 pre-encounter maneuver.

The E6 post-encounter reconstruction (**OD159**) showed that the spacecraft missed its target by 9.7 km, 2.3 km and -2.8 seconds along the R component, the T component and in time from closest approach. The flyby differed from the pre-encounter solution (**OD156**) by 1.1σ in R, 1.3σ in T and 1σ in TCA. Europa's ephemeris shifted 2σ (6.1 km) in downtrack from the pre-E6 ephemeris. Only 58% of the scheduled OPNAVs were successful for the E6 encounter.

Table 6: Orbit Determination Solutions Supporting the E6 Encounter on 20 February 1997

OD	OTM	DCO	B•R (km)	B•T (km)	TCA (SCET UTC)	σ SMA (km)	σ SMI (km)	Θ (deg)
Target			614.6	-2170.2	17:06:13.0			
OD153	18	E6-53d	688.8 \pm 13.1	-3297.9 \pm 189.2	17:14:51.5 \pm 67.4	189.2	12.6	1.1
OD155	19	E6-17d	689.3 \pm 8.6	-3036.3 \pm 6.2	17:13:16.3 \pm 2.6	8.6	6.2	91.0
OD156	20	E6-4d	615.4 \pm 8.2	-2164.1 \pm 2.4	17:06:09.2 \pm 0.7	8.2	2.4	89.6
OD159	21	E6+10h	624.3 \pm 0.2	-2167.9 \pm <0.05	17: 06:10.2 \pm <0.05	0.2	<0.05	90.9
OD163	22	E6+Apo	624.2 \pm 0.2	-2167.9 \pm <0.05	17: 06: 10.2 \pm <0.05	0.2	<0.05	93.8

G7 Approach & Encounter (Refer to Figure 9 and Table 7)

The E6 post-encounter maneuver OTM-21 was performed 3.5 days after the E6 encounter, raising the orbit

period by 32 minutes with a ΔV of 0.9 m/s. This orbit of Jupiter included a distant Io occultation on the outbound leg. An apojove maneuver (OTM-22) was required after the occultation to return the spacecraft to the trajectory necessary to continue the tour. OTM-22 was implemented at apojove on 13 March 1997 with a ΔV of 15.76 m/s \pm 0.075%. This maneuver contained a significant out-of-plane component, a direction insensitive to radiometric reconstruction efforts. Any maneuver execution errors in OTM-22 therefore propagated forward to the upcoming encounter (mostly in the R component).

The optical data for the pre-encounter maneuver consisted of eight opnavs, all scheduled within 1.5 days of the data cutoff (March 30). All eight were successful, including a pair of Io/Ganymede images. (The remaining six captured only Ganymede). The utility of these frames was the gain in information for the out-of-plane components of OTM-22 and Ganymede (the downtrack component of Ganymede was already well determined from G1 and G2). The resulting solution (**OD165**) showed a 25 km shift in B•R for Ganymede. The *a priori* satellite covariance for G7 was derived from the G1 through E6 encounters.

The miss with respect to the target was -2.1 km in B•R, -9.8 km in B•T, and -0.2 seconds in TCA, corresponding to errors of 0.24σ in B•R, 0.47σ in B•T, and 0.4σ in TCA. The Ganymede changes between the pre- and post-encounter solutions were 0.1 km, 3.9 km, and 2.9 km in the radial, downtrack, and normal directions, respectively, corresponding to errors of 0.1σ , 0.6σ , and 1.3σ . The small satellite ephemeris corrections validated the use of G1 and G2 encounter information to predict the ephemeris seven months in advance.

Table 7: Orbit Determination Solutions Supporting the G7 Encounter on 5 April 1997

OD	OTM	DCO	B•R (km)	B•T (km)	TCA (SCET UTC)	σ SMA (km)	σ SMI (km)	Θ (deg)
Target			-4842.0	-3318.7	07:09:58.3			
OD159	21	E6+10h	-4827.6 \pm 5.6	-21421.1 \pm 94.7	06:31:46.2 \pm 11.4	94.7	5.1	178.6
OD163	22	G7-31d	-11865.9 \pm 5.3	-51270.6 \pm 18.4	05:55:28.6 \pm 2.0	18.4	5.2	178.4
OD164	-	G7-16d	-4822.8 \pm 23.0	-3087.4 \pm 18.3	07:10:35.0 \pm 1.6	23.6	17.5	71.1
OD165	23	G7-6d	-4847.5 \pm 8.6	-3087.4 \pm 7.1	07:10:35.0 \pm 0.2	8.7	6.9	107.5
OD167	24	G7+11h	-4844.1 \pm <0.05	-3328.5 \pm <0.05	07:09:58.1 \pm <0.05	<0.05	<0.05	54.9
OD169	25	G7+Apo	-4844.1 \pm <0.05	-3328.5 \pm <0.05	07:09:58.1 \pm <0.05	<0.05	<0.05	58.4

G8 Approach & Encounter (Refer to Figure 10 and Table 8)

OTM-24 was performed three days after G7, reducing the orbit period by 9 minutes with a ΔV of 0.6 m/sec. The post-encounter maneuver (intentionally) corrected all but 250 km of the distance to the target in the G8 B-plane, with the remainder left to the apojove maneuver.

The G8 approach was the first encounter navigated without optical information (although the eight G7 OPNAV's were still within the data arc for the G8 solution). Nevertheless, the small magnitude of OTM-24 and OTM-25, combined with the repeat visit to Ganymede, augured small B-plane errors. As it turned out, the encounter miss with respect to the target was only -0.45 km in B•R, -8.4 km in B•T, and 0.25 seconds

in TCA. (The pre-encounter maneuver was not needed and was cancelled.) The difference from the pre-encounter maneuver design (**OD170**) were 0.3 km in B•R, -4.3 km in B•T, and 0.04 seconds in TCA corresponding respectively, to errors of 0.2σ , 2.4σ , and 0.4σ . The ephemeris uncertainty of Callisto during the non-targeted encounter with Callisto preceding G8 (C8a) contributed to the magnitude of the B•T miss. The Ganymede ephemeris differences between **OD170** and **OD172** were 0.005 km, 0.41 km, and 0.29 km in the radial, downtrack, and normal directions, respectively, corresponding to errors of 0.15σ , 0.6σ , and 0.2σ .

Table 8: Orbit Determination Solutions Supporting the G8 Encounter on 7 May 1997

OD	OTM	DCO	B•R (km)	B•T (km)	TCA (SCET UTC)	σ SMA (km)	σ SMI (km)	Θ (deg)
Target			-2058.0	-3853.2	15:56:09.3			
OD167	24	G7+11h	-2991.7 \pm 9.6	-12515.3 \pm 71.1	16:10:54.0 \pm 7.2	71.8	1.4	7.6
OD169	25	G8-23d	-2029.7 \pm 1.8	-4082.5 \pm 13.7	15:56:45.7 \pm 1.4	13.8	1.2	5.7
OD170	26	G8-5d	-2058.7 \pm 1.3	-3857.3 \pm 1.8	15:56:09.5 \pm 0.1	1.8	1.3	2.1
OD171	-	G8-1d	-2059.1 \pm 1.3	-3861.0 \pm 0.9	15:56:09.5 \pm 0.1	1.3	0.9	93.2
OD172	27	G8+4h	-2058.4 \pm <0.05	-3861.6 \pm <0.05	15:56:09.5 \pm <0.05	0.1	<0.05	139.5
OD175	28	G8+Apo	-2058.4 \pm <0.05	-3861.6 \pm <0.05	15:56:09.5 \pm <0.05	0.1	<0.05	140.6

C9 Approach & Encounter (Refer to Figure 11 and Table 9)

The post-encounter maneuver OTM-27 was performed 3.5 days after G8, increasing the orbit period by 49.5 minutes with a ΔV of 0.9 m/sec. Similar to OTM-24, the maneuver was designed to correct all but 75 km of C9 B-plane error, leaving the remainder to be removed at apojove where it could be removed more efficiently. The pre-encounter maneuver, OTM-29, was found to be unnecessary and was cancelled.

Based on 12 days of data following C9, **OD181** showed that the C9 encounter missed the target by 0.9 km in B•R, -3.0 km in B•T, and 0.03 seconds in TCA. Compared to the pre-encounter maneuver solution (**OD177**), the errors were 0.7σ in B•R, 1.3σ in B•T, and 0.75σ in TCA. The Callisto ephemeris differences between **OD177** and **OD181** were -0.44 km, 1.48 km, and -0.12 km in the radial, downtrack, and normal directions, respectively, corresponding to errors of 0.96σ , 2.0σ , and 0.04σ . Although the errors were 2σ in downtrack and 1.3σ in crosstrack, the sigmas were small in absolute magnitude.

Table 9: Orbit Determination Solutions Supporting the C9 Encounter on 25 June 1997

OD	OTM	DCO	B•R (km)	B•T (km)	TCA (SCET UTC)	σ SMA (km)	σ SMI (km)	Θ (deg)
Target			-65.3	-2930.1	13:47:49.9			
OD172	27	G8+4h	-384.3 \pm 1.6	20620.2 \pm 72.5	13:08:38.4 \pm 7.2	72.5	1.4	179.3
OD175	28	C9-30d	-78.0 \pm 1.4	-2768.3 \pm 7.4	13:47:22.9 \pm 0.8	7.4	1.4	179.5
OD177	29	C9-7d	-65.4 \pm 1.4	-2931.7 \pm 1.0	13:47:49.9 \pm 0.1	1.4	1.0	92.9

OD181 30 C9+12d -64.4 ± 0.6 -2933.1 ± <0.05 13:47:50.0 ± <0.05 0.6 <0.05 91.5

C10 Approach & Encounter (Refer to Figure 12 and Table 10)

The post-encounter maneuver OTM-30 was performed 15 days after C9, increasing Galileo's orbit period by 44.5 minutes with a ΔV of 1.2 m/sec. This maneuver was designed to partially correct the C10 B-plane errors and to target the spacecraft into a position at apojove from which to observe a sequence of Io occultations of Earth.

Galileo missed the C10 target by 4.5 km in B•R, -3.4 km in B•T, and 0.0 seconds in TCA as determined by **OD187**. Compared to the pre-encounter maneuver design solution (**OD185**), the errors at the B-plane were 0.5σ in B•R, 2.3σ in B•T, and 0σ in TCA. (The pre-encounter maneuver OTM-32 was cancelled because the spacecraft trajectory prediction was already subsigma with respect to the target). The Callisto ephemeris changed between subsequent encounters (**OD183** cf. **OD187**) by -0.12 km, -0.2 km, and -1.48 km in the radial, downtrack, and normal directions, respectively, corresponding to errors of 3σ, 4σ, and 0.6σ with respect to the **OD183** uncertainties. Although the ephemeris errors were significant in a relative sense, the absolute excursions were small. The satellite model was not expected to retain fidelity at sub-kilometer precisions.

Table 10: Orbit Determination Solutions Supporting the C10 Encounter on 17 September 1997

* time on 16 September 1997

OD	OTM	DCO	B•R (km)	B•T (km)	TCA (SCET UTC)	σSMA (km)	σSMI (km)	Θ (deg)
Target			-283.6	3040.2	00:18:54.8			
OD181	30	C9+12d	-749.8 ± 5.2	27382.6 ± 92.8	23:42:00.5*± 10.1	92.9	5.1	179.2
OD183	31	C9+32d	-249.2 ± 6.8	-282.5 ± 32.7	00:25:42.2± 4.2	32.7	6.8	179.3
OD185	--	C10-6d	-284.6 ± 8.6	3040.5 ± 1.5	00:18:54.5± 4.2	8.6	1.5	88.9
OD186	33	C10+3h	-287.5 ± 0.3	3036.9 ± 0.03	00:18:54.8± <0.01	0.3	0.02	84.9
OD187	--	C10+7d	-288.1 ± 0.2	3036.8 ± 0.02	00:18:54.8± <0.01	0.2	0.01	84.8

E11 Approach & Encounter (Refer to Figure 13 and Table 11)

The post-encounter maneuver OTM-33 was performed three days after C10, decreasing the orbit period by two hours with a ΔV of 0.9 m/sec. This maneuver was designed to partially correct the trajectory errors incurred at the C10 encounter, with the remainder to be corrected at apojove. OTM-34 corrected apojove errors as well as implementing a deterministic adjustment to the trajectory.³ OTM-34 occurred on 18 October, 1997 with a ΔV of 14.47 m/s ± 0.090%.

The E11 reconstruction, **OD192**, using seven hours of post-encounter data, showed that the spacecraft missed its target by -18.9 km in B•R, -8.0 km in B•T, and 0.0 seconds in TCA. Compared to the pre-encounter maneuver design (**OD189**), the errors were 3.4 km in B•R, 1.4 km in B•T, and 0 s in TCA. Europa changed by 6.3 km, 6.6 km, and 20.4 km in the radial, downtrack, and normal directions,

respectively (**OD187** cf. **OD192**), corresponding to substantial formal errors with respect to **OD187**. The magnitudes of these errors were small compared to JUP088, however, and were anticipated since E11 was not immediately preceded by another encounter with Europa. Without up-to-date Doppler and optical information, the state of Europa was not directly determinable and resulted in significant uncertainty at encounter time (*i.e.* on the order of JUP088 uncertainty).

Table 11: Orbit Determination Solutions Supporting the E11 Encounter on 6 November 1997
* time on 7 November 1997

OD	OTM	DCO	B•R (km)	B•T (km)	TCA (SCET UTC)	σ SMA (km)	σ SMI (km)	Θ (deg)
Target			-1553.6	3365.9	20:31:44.2			
OD186	33	C10+3h	-2708.2 \pm 28.6	-13173.1 \pm 24.9	02:56:43.6* \pm 68.5	27.1	24.4	64.6
OD187	--	C10+7d	-2870.7 \pm 4.2	-12836.4 \pm 14.1	00:58:51.1* \pm 16.4	14.1	4.1	177.5
OD188	34	C10+26d	-2870.4 \pm 3.5	-12849.2 \pm 1.6	00:58:59.2* \pm 4.9	3.5	1.6	92.0
OD189	35	E11-13d	-1551.9 \pm 5.6	3240.3 \pm 5.9	20:32:21.6 \pm 2.9	6.0	5.5	166.1
OD192	36	E11+7h	-1572.7 \pm 0.06	3357.9 \pm 0.04	20:31:44.2 \pm 0.003	0.06	0.01	57.3

E12 Approach & Encounter (Refer to Figure 14 and Table 12)

The E11 post-encounter maneuver OTM-36 was performed three days after E11, increasing the orbit period by 34 minutes with a ΔV of 2.1 m/sec. This maneuver was designed to partially correct the trajectory errors incurred at the E11 encounter, with the remainder to be corrected at apojoove.

Using seven hours of data after E12, solution **OD197** showed that the spacecraft missed the E12 target by 1.0 km in B•R, 0.8 km in B•T, and 0.1 seconds in TCA. Compared to the pre-encounter maneuver design solution **OD195**, the errors were 0.4σ in B•R, 0.7σ in B•T, and 0.3σ in TCA. The Europa ephemeris changed by 20 m, 200 m, and 1.9 km in the radial, downtrack, and normal directions, respectively (**OD194** cf. **OD197**), corresponding to 0.7σ in radial, 0.6σ in downtrack, and 1.5σ in timing errors with respect to **OD194**. The magnitudes of these errors were expected since E12 was immediately preceded by another Europa encounter. The E11 encounter information reduced Europa's mean motion error to negligible levels.

Table 12: Orbit Determination Solutions Supporting the E12 Encounter on 16 December 1997

OD	OTM	DCO	B•R (km)	B•T (km)	TCA (SCET UTC)	σ SMA (km)	σ SMI (km)	Θ (deg)
Target			269.7	1831.6	12:03:20.0			
OD192	36	E11+7h	-11167.8 \pm 24.3	109767 \pm 109.6	11:38:26.8 \pm 44.1	112.2	4.7	12.3
OD194	37	E11+13d	344.3 \pm 2.9	2357.9 \pm 7.9	12:12:01.5 \pm 5.4	8.0	2.7	7.8
OD195	38	E12-7d	274.8 \pm 2.4	1826.6 \pm 1.1	12:03:12.0 \pm 0.3	2.5	0.9	104.3
OD197	39	E12+7h	270.7 \pm 0.1	1832.4 \pm 0.01	12:03:19.9 \pm 0.001	0.1	0.01	92.8

Satellite Ephemeris Improvement

The Galilean satellite orbits were known to approximately 50 km RSS ($1-\sigma$) at the time of Galileo's arrival.⁶ With Galileo data, knowledge of the satellite ephemerides improved by two to three orders of magnitude at encounter locations (times) and approximately one order of magnitude elsewhere [*i.e.* to better than five km as of January 1, 1998 (less than one km for Europa and Ganymede)]. The continuous improvement of the satellite ephemeris as the tour progressed has contributed to the overall navigation performance of Galileo.

Table 13 illustrates the incremental position change occurring between subsequent encounters. Relatively large movements took place early in the tour, after the first and/or second encounter with each respective satellite. One exception to this pattern was E11, where a change of 22 km RSS occurred close to the end of the nominal tour. Uncertainty in Europa's node caused that out-of-plane shift, occasioned by a dearth of recent data. To contrast, Ganymede and Callisto ephemerides had retained currency with occasional non-targeted flybys interspersed throughout the tour (see Table 1). For E11, without optical information, the last direct position information of Europa was nine months earlier at E6.

Table 13: Satellite Ephemeris Differences Between Subsequent Encounters

Ephemerides Compared	Enc	Satellite	ΔR (km)	ΔT (km)	ΔN (km)	Respective Data Arcs
OD128 - JUP088	G1	Ganymede	-16.99	-39.25	-1.98	G1+Apo - <i>a priori</i>
OD137 - OD128	G2	Ganymede	0.20	-8.13	6.57	G2+Apo - G1+apo
OD145 - OD137	C3	Callisto	-2.04	-23.84	15.41	C3+Apo - G2+apo
OD155 - OD145	E4	Europa	-1.40	16.08	17.38	E5A+Apo - C3+apo
OD163 - OD155	E6	Europa	-0.17	7.54	-0.98	E6+Apo - E5A+apo
OD169 - OD163	G7	Ganymede	-0.13	-3.91	3.73	G7+Apo - E6+apo
OD175 - OD169	G8	Ganymede	-0.03	0.40	0.21	G8+Apo - G7+apo
OD181 - OD175	C9	Callisto	-0.41	1.49	-0.12	PostC9 - G8+apo
OD187 - OD181	C10	Callisto	-0.07	0.20	-1.57	PostC10 - PostC9
OD192 - OD187	E11	Europa	6.31	6.64	20.4	PostE11 - PostC10
OD197 - OD192	E12	Europa	-0.02	-0.32	-2.13	PostE12 - PostE11

An indication of the overall ephemeris improvement is illustrated in Table 14. Table 14 compares a JUP088 satellite state with a state from the OD200 satellite ephemeris of January 1998 (ephemerides compared on January 1, 1998), as well as showing the corresponding improvement in our assessment of the accuracy of that knowledge (*i.e.* the ephemeris uncertainty). The adjustments are all sub-sigma with respect to JUP088.

Table 14: Satellite Ephemeris Differences for the Epoch January 1, 1998

(OD200 versus JUP088)

	Δ Position at Epoch (km, RSS)	Δ Velocity at Epoch (cm/s, RSS)	Position Uncertainty as of Nov, 1995 (JUP088) (km, RSS)	Position Uncertainty at Epoch (OD200) (km, RSS)
Io	7	5	± 42	± 4.9
Europa	54	110	± 80	± 0.6
Ganymede	28	45	± 78	± 0.9
Callisto	55	23	± 50	± 3.8

Jupiter Ephemeris Improvement

Prior to Ganymede-1 we found that the Jupiter ephemeris computed from **OD120** (eph-OD120) had shifted 316 km in the out-of-plane component and -5 km downtrack with respect to an ephemeris computed at the time of Jupiter arrival (six months earlier). In retrospect the earlier ephemeris (eph-OD105) was not sufficiently sensitive to Jupiter's out-of-plane component (minimal data acquired after the Jupiter encounter) although eph-OD105 too had shifted significantly with respect to the baseline ephemeris DE-143. Solution **OD120** shifted more in the out-of-plane component than **OD105** because of the additional six months of post-encounter data and a spacecraft orbit inclined to Jupiter's equator. The overall change of eph-OD120 from DE-143 at the time of the Jupiter encounter (Dec. 7, 1995) was determined to be 18 km radial, -77 km downtrack, and 372 km out-of-plane. Table 15 lists Jupiter's ephemeris changes with respect to DE-143 and the 1- σ uncertainties at the time of the G1 encounter.

Table 15: Jupiter Ephemeris Differences with respect to the JPL Ephemeris DE-143*

Ephemerides Compared	Orbit	ΔR (km)	ΔT (km)	ΔN (km)	ΔDR (mm/s)	ΔDT (mm/s)	ΔDN (mm/s)
OD105	JOI	16.54 ± 1.37	-72.53 ± 11.3	56.27 ± 179.1	1.15	-0.18	-1.18
OD120	G1	18.02 ± 1.77	-77.46 ± 10.2	372.06 ± 76.20	1.25	-0.19	-5.31
OD133	G2	18.41 ± 2.02	-77.89 ± 4.80	457.64 ± 58.44	1.25	-0.20	-6.40
OD138	C3	17.88 ± 2.31	-70.67 ± 9.72	370.72 ± 58.98	1.12	-0.20	-5.14
961127†	G2-C3	16.36 ± 3.87	-75.81 ± 8.93	259.58 ± 57.31	1.20	-0.17	-3.86
OD166	G7	13.98 ± 4.07	-71.25 ± 4.61	304.96 ± 37.71	1.15	-0.14	-4.46
OD185	C10	18.60 ± 4.11	-96.05 ± 5.60	238.46 ± 21.73	1.42	-0.21	-5.44

*Heliocentric Earth-Mean-Ecliptic of 1950, Jupiter-Orbit fixed, at the time of the G1 encounter

†Includes 2 east-west, and 2 north-south VLBI measurements

Further observations undertaken with Very Long Baseline Interferometry (VLBI) measurements from July through September 1996 obtained four points -- two east-west and two north-south measurements. VLBI data establishes plane-of-sky position of the spacecraft. The resulting ephemeris, eph-961127, agreed with eph-OD120 in the radial and downtrack components and reduced the out-of-plane shift by -112 km, but did not significantly improve the overall certainty in Jupiter's state. Apparently the out-of-plane component

has resisted precise determination because long uninterrupted arcs are required to accurately infer state along that component.¹¹ Galileo arcs, including maneuvers and encounters, cannot be considered 'uninterrupted' and consequently provide poor insight into out-of-plane components. Additional VLBI measurements were acquired over the next year, but the ephemerides produced with those later data did not differ significantly from the ephemerides produced with Doppler-only solutions. Figure 15 illustrates the topology of all Galileo VLBI measurements obtained in the Jovian system.

Gravity Field Estimates of the Jovian System

Figure 16 illustrates changes in the Galilean satellite masses (GM) from *a priori* values as a function of time (June 27, 1996 - December 27, 1997). Also shown are changes in Jupiter's mass (divided by 100) from the *a priori*. The *a posteriori* 1- σ uncertainties for these mass estimates are shown in Figure 17. Improvements in ephemeris knowledge after each flyby are evident in Figure 17, particularly for the *encountered* satellite. The ephemeris covariance was scaled by three during solar conjunction (January 1997), so Figure 17 shows an increase in all mass uncertainties at that time. The sudden improvement of Europa's mass after the C3 encounter can be attributed to the E3A non-targeted flyby (see Table 1). The sudden improvement of Io's mass after C10 can be attributed to a close passage of Io (but at a distance greater than 100,000 km and so this encounter is not noted in Table 1). Together, Figures 16 and 17 illustrate the consistency of mass estimates for Ganymede, Europa and Callisto since the C3 encounter. Note that Jupiter's mass estimate underwent roughly three levels of changes: between G1 and G2 ($\sim 40 \text{ km}^3/\text{s}^2$), between G2 and E4 ($\sim +50 \text{ km}^3/\text{s}^2$) and after E6 ($\sim 10 \text{ km}^3/\text{s}^2$). (We have not investigated whether ephemeris updates or scaling could have influenced these groupings.)

Table 16 lists the masses, oblateness, and other relevant parameters of the Jovian system, using the last post-encounter solution of E12 (OD200) as the current best estimate. Jupiter's low order oblateness terms (J2,J4) have not improved significantly from the *a priori*; all other terms in Table 16 *have* improved significantly from the *a priori*.¹³

The satellite gravity field estimates tabulated in Table 16 have not previously been obtained. Analysis of these gravity fields indicates that Ganymede and Europa have differentiated into predominantly three layers: an outer water shell approximately 100 km thick and an interior of rocky material with possibly a metallic core.¹⁴ Parts (or most) of Europa's outer shell could be liquid water, with just a thin water ice lithosphere floating on the liquid. High resolution images of Europa supply indirect corroborating evidence of a global ocean -- showing a terrain nearly crater-free and of low relief, with a surface apparently undergoing constant re-working.¹⁵ Callisto has not differentiated as completely as Europa and Ganymede, consisting of only two layers (water ice and rock). Moreover Callisto has one of the most densely cratered surfaces in the solar system.

Sufficient heat to maintain a global liquid ocean on Europa can be supplied by tidal dissipation.¹⁶ Tidal heating can originate from the torques acting on satellites in eccentric orbits (for Europa, $e = 0.009$), flexing the satellites and causing rotation to be non-synchronous.

Table 16: Estimates of the Jovian Masses (km^3/s^2), Gravity, and Pole Orientation (EME-50)

Jupiter				
Gravity				
GM	126,712,764.99 \pm 2.51			
J2 ($\times 10^{-6}$)	14,737.05 \pm 0.96			
J4 ($\times 10^{-6}$)	-587.80 \pm 5.00			
Pole (EME-50)				
R.A. (deg)	268.0007 \pm 0.0006			
Dec (deg)	64.5053 \pm 0.0003			
Satellites	Io	Europa	Ganymede	Callisto
GM	5959.91 \pm 0.11	3202.72 \pm 0.01	9887.81 \pm 0.01	7179.26 \pm 0.02
J2 ($\times 10^{-6}$)	1863 \pm 423	441 \pm 20	146 \pm 23	25 \pm 10
C22 ($\times 10^{-6}$)	547 \pm 14	132 \pm 1	33 \pm 5	7 \pm 3
S22 ($\times 10^{-6}$)	19 \pm 12	-9 \pm 1	3 \pm 5	-1 \pm 3

Summary of Results

A comparison of the achieved navigation results with our predictions are tabulated in Table 17. Except for the first encounter (for which predictions closely matched the achieved values), the predicted errors were conservative vis-a-vis the achieved results. We attribute this to our observation that the actual uncertainty for maneuvers was significantly smaller than predicted by the propulsion system designers, as well as for the following factors: 1) our successful use of Doppler data within one hour of an encounter (this had not previously been assumed), and 2) our successful use of satellite covariances derived from previous encounters. Selected navigation solutions supporting the eleven satellite encounters are listed in Table A-2.

For the first dozen orbits, the average trajectory errors in delivering Galileo to its targeted *aimpoints* were 0.9σ in B•R, 0.6σ in B•T, and 1.6σ in encounter time (with respect to the pre-encounter solution). Sub-sigma deviations from the target resulted at the E4, E6, G7 and G8 encounters. The E11 encounter experienced the largest relative position error of 3.4σ in B•R (the pre-encounter solution was computed six days earlier than for all previous encounters, and a dearth of optical navigation), but the timing of the encounter was precise with a relative error in TCA of 0.0σ .

Overall, errors between the pre-encounter solution and the *reconstruction* remained less than 20 km in B•R, 22 km in B•T and 8 sec in TCA for the eleven encounters (except E11 with a TCA error of 37 seconds, for the same reasons given above). As seen with several encounters, fidelity of the satellite model was lost when sub-kilometer precision was predicted.

The total propellant expended to navigate the eleven satellite tour [from OTM-4 (perijove raise maneuver) to OTM-39 (post-E12)] was equivalent to a ΔV of 58.8 m/s (including the propellant necessary for attitude

Table 17
Table 1. Predicted Tour OD

OTM	Time of Maneuver	Data Cutoff	B•R (km)			B•T (km)			TCA (s)		
			Achieved	1993‡	1996¶	Achieved	1993‡	1996¶	Achieved	1993‡	1996¶
4	PJR + 57d		94.1	-	-	342.5	-	-	47.5	-	-
5	G1 - 15d	G1 - 21d 19:55	73.2	-	-	48.0	-	-	5.1	-	-
6	G1 - 2.4d	G1 - 3d 13:36	16.3	12.7	15.0	30.5	25.0	21.0	1.7	1.8	1.0
	G1	Reconstruction	0.1			0.1			<0.05		
7	G1 + 3.1d	G1 + 0d 09:54	-	98.2	-	-	3349.7	-	-	409.0	-
8	G1 + Apo	G2 - 42d 12:41	7.0	1.4	-	22.0	34.4	-	2.9	4.2	-
9	G2-10d	G2 - 18d 11:49	6.8	-	-	21.5	-	-	2.9	-	-
10	G2 - 2d	G2 - 3d 06:11	3.0	9.9	9.0	6.9	23.9	3.0	0.3	0.9	0.2
	G2	Reconstruction	0.5			0.4			<0.05		
11	G2 + 3.1d	G2 + 0d 11:19	22.5	61.0	-	399.1	3056.1	-	39.4	310.0	-
12	G2 + Apo	C3 - 37d 17:04	26.3	43.0	-	47.0	79.9	-	3.4	4.1	-
13	C3 - 3d	C3 - 4d 11:01	15.9	18.6	19.0	34.6	29.5	42.0	1.6	1.3	1.6
	C3	Reconstruction	0.1			0.0			<0.05		
14	C3 + 5.7d	C3 + 1d 04:45	18.6	53.3	-	2142.4	3125.4	-	495.4	1270.2	-
15	C3 + Apo	E4 - 30d 13:16	15.9	21.5	-	12.3	21.8	-	4.0	6.9	-
16	E4 - 3.1d	E4 - 4d 17:45	11.3	8.4	10.0	4.7	10.3	5.0	1.9	2.5	1.6
	E4	Reconstruction	1.5			0.1			<0.05		
17	E4 + 4.2d	E4 + 0d 19:14	-	36.5	-	-	1986.0	-	-	668.9	-
18	E4 + Apo	E6 - 53d 01:25	13.1	-	-	189.2	-	-	67.4	-	-
19	Orbit 5 Apo	E6 - 17d 04:42	8.6	89.4	-	6.2	36.0	-	2.6	13.4	-
20	E6 - 2d	E6 - 4d 04:25	8.0	11.9	13.0	3.0	10.5	3.0	1.0	0.5	0.7
	E6	Reconstruction	0.2			0.0			<0.05		
21	E6 + 3.5d	E6 + 0d 09:52	5.7	41.0	-	99.2	400.1	-	11.9	57.4	-
22	E6 + Apo	G7 - 31d 09:58	5.3	38.8	-	18.4	47.1	-	2.0	3.3	-
23	G7 - 4d	G7 - 6d 02:07	8.7	8.0	20.0	9.3	20.6	16.0	0.5	1.7	0.6
	G7	Reconstruction	<0.05			0.0			<0.05		
24	G7 + 3d	G7 + 0d 11:02	9.6	31.4	-	71.1	273.5	-	7.2	26.6	-
25	G7 + Apo	G8 - 23d 04:18	1.9	15.3	-	14.1	68.8	-	1.5	6.1	-
26	G8 - 2.7d	G8 - 5d 01:40	1.3	26.2	10.0	1.8	28.6	17.0	0.1	1.2	0.2
	G8	Reconstruction	<0.05			0.1			<0.05		
27	G8 + 3.5d	G8 + 0d 04:20	1.6	13.5	-	72.5	367.9	-	7.2	35.4	-
28	G8 + Apo	C9 - 29d 20:03	1.4	20.1	-	7.4	12.4	-	0.8	2.0	-
29	C9 - 2.2d	C9 - 6d 21:38	1.4	34.4	7.0	1.0	53.9	8.0	0.1	2.2	0.8
	C9	Reconstruction	0.7			<0.05			<0.05		
30	C9 + 15d	C9 + 12d 1h	5.2	33.7	-	92.8	1697.7	-	10.1	177.0	-
31	C9 + Apo	C10 - 50d 11h	6.8	4.5	-	32.7	22.1	-	4.2	2.9	-
32	C10 - 3d	C10 - 6d 3h	8.6	20.7	11.0	1.5	32.7	7.0	0.7	1.8	0.4
	C10	Reconstruction	0.3			<0.05			<0.05		
33	C10 + 3.9d	C10 + 0d 3h	26.6	249.7	-	24.9	125.2	-	68.5	57.8	-
34	C10 + Apo	E11 - 24d 17h	3.5	43.0	-	1.6	17.7	-	4.9	6.5	-
35	E11 - 3d	E11 - 12d 20h	5.6	9.6	20.0	5.9	6.9	8.0	2.9	2.5	2.5
	E11	Reconstruction	<0.06			<0.05			<0.05		
36	E11 + 3.9d	E11 + 0d 7h	24.3	-	-	109.6	-	-	44.1	-	-
37	E11 + Apo	E12 - 26d 17h	2.9	-	-	7.9	-	-	5.4	-	-
38	E12 - 3d	E12 - 6d 16h	2.4	-	-	1.1	-	-	0.3	-	-
	E12	Reconstruction	0.1			<0.05			<0.05		

‡Haw et al. [1993]

¶D'Amaro et al. [1996]

maintenance and pointing turns). This total included a 14 m/s apojove maneuver following C10 which was not part of the original tour design, but which was later discovered to be necessary in order for the tour to be extended beyond E12.³ Compare this to a ΔV of ~ 100 m/s originally anticipated for the tour (not including E12, which was not part of the original design).⁴ During the first dozen orbits, the mean maneuver magnitude underperformed by 0.3%, and the average pointing excursion deviated 0.08% from the *a priori*. As of January 1, 1998, an equivalent velocity change of approximately 50 m/s remained on-board, sufficient propellant for three additional years of spacecraft operation.

By April, 1997 (after six encounters), satellite locations were known to less than 10 km ($1-\sigma$). At this level of accuracy the remainder of the mission could operate without optical navigation, since the contribution of optical data to ephemeris improvement had become insignificant. Along with ephemeris improvement, knowledge of the satellite masses improved significantly also. Gravitational parameters are now known to better than $2 \text{ km}^3/\text{s}^2$ for Io, $0.1 \text{ km}^3/\text{s}^2$ for Europa, $0.2 \text{ km}^3/\text{s}^2$ for Ganymede and $0.1 \text{ km}^3/\text{s}^2$ for Callisto, factors of 5, 100, 15 and 30, respectively better than the masses determined from the Voyager and Pioneer missions. Gravity fields for each of the major moons have been determined for the first time. The gravity of Jupiter has been determined to better than $10 \text{ km}^3/\text{s}^2$ which is a factor of 10 better than previous knowledge. In addition, errors in the EME-1950 pole of Jupiter have been improved by a factor of three to eight.

Large shifts ($>1-\sigma$) in Jupiter's ephemeris on the order of 70 km in downtrack and 300 km in the out-of-plane direction have been observed with respect to the JPL planetary ephemeris DE-143. The Galileo project decided in 1978 to use the B1950 system, so inconsistencies between this coordinate frame and the standard J2000 frame may exist. Further study is needed to understand these changes.

The OPNAV campaign, revised to accommodate the capability of the low gain antenna, finished in April 1997 with a 64% success rate. Many unsuccessful OPNAVs were the result of low tolerance viewing opportunities created by the pre-encounter attitude maintained by the spacecraft.

Concluding Remarks

Accurate propagations were achieved for Galileo by incorporating increased knowledge of satellite mean motion into the trajectory model. This resulted in the cancellation of five of eleven pre-encounter maneuvers. The resulting propellant savings may lead to as much as a four year extension of the Galileo mission.

For the first time, gravity field measurements were obtained for the Galilean moons of Jupiter. As discussed, substantial quantities of liquid water may exist on Europa beneath an external ice shell.

Galileo operations in Jupiter orbit are expected to continue through 1999.

Acknowledgement

The work described in this paper was performed at the Jet Propulsion Laboratory, California Institute of Technology, under a contract with NASA. The authors would like to express their gratitude to the

following individuals for their contribution to the navigation effort: Robert Jacobson for producing the *a priori* satellite ephemeris and Michael Wang for software and OPNAV support.

References

1. Antreasian, P.G., Nicholson, F.T., Kallemeyn, P.H., Bhaskaran, S., Haw, R.J., Halamek, P., "Galileo Orbit Determination for the Ida Encounter." *Advances in the Astronautical Sciences* 1994, Vol. 87, Part 2, pp. 1027-1048, Univelt, San Diego, California, 1994.
2. Antreasian, P.G., McElrath, T.P., Haw, R.J., Lewis, G.D., "Galileo Orbit Determination Results During the Satellite Tour", Paper AAS-97-699, *AAS/AIAA Astrodynamics Specialist Conference*, Sun Valley, Idaho, August 4-7, 1997.
3. Bell, J.L., Johannesen, J.R., "Galileo Europa Mission (GEM) Tour Design," Paper AAS-97-614, *AAS/AIAA Astrodynamics Specialist Conference*, Sun Valley, Idaho, August 4-7, 1997.
4. D'Amario, L.A., Byrnes, D.V., Haw, R.J., Kirhofer, W.E., Nicholson, F.T., and Wilson, M.G., "Navigation Strategy for the Galileo Jupiter Encounter and Orbital Tour," *Astrodynamics 1995: Proceedings of the AAS/AIAA Astrodynamics Specialist Conference*, pp. 1387-1411, Univelt, San Diego, CA, 1996.
5. Haw, R.J., Kallemeyn, P.H., Nicholson, F.T., Davis, R.P., Riedel, J.E., "Galileo Satellite Tour: Orbit Determination," *AAS/AIAA Astrodynamics Specialist Conference*, Victoria, B.C., Canada, August 16-19, 1993, Paper AAS-93-686.
6. Haw, R.J., Antreasian, P.G., Graat, E.G., McElrath, T.P., Nicholson, F.T., "Navigating Galileo at Jupiter Arrival," *Journal of Spacecraft and Rockets*, Vol. 34, No. 4, pp. 503-508, July-August, 1997.
7. Kallemeyn, P.H., R.J. Haw, V.M. Pollmeier, F.T. Nicholson, "Galileo Orbit Determination for the Gaspra Encounter," Paper AAS-92-4523, *AIAA/AAS Astrodynamics Conference*, Hilton Head, South Carolina, August 10-12, 1992.
8. Wilson, M.G., Potts, C.L., Mase, R.A., Halsell, C.A., Byrnes, D.V., "Maneuver Design for Galileo Jupiter Approach and Orbital Operations," *International Symposium on Spacecraft Dynamics*, Darmstadt, Germany, June 2-6, 1997.
9. Wolf, A.A., Byrnes, D.V., "Design of the Galileo Satellite Tour," *AAS/AIAA Astrodynamics Conference*, Victoria, B.C., August 16-19, 1993, AAS-93-567.
10. Murrow, D.W., Jacobson, R.A., "Galilean Satellite Ephemeris Improvement Using the Galileo Tour Encounter Information," *AIAA/AAS Astrodynamics Conference*, Minneapolis, Minnesota, August 15-17, 1988, AIAA-88-4249.
11. Seife, C., "Distant Spacecraft Seem to be Showing No Respect for the Laws of Physics," *New Scientist*, London UK, Issue 12, September 1998, p.4.

12. Hamilton, T.W., Melbourne, W.G., "Information Content of a Single Pass of Doppler Data from a Distant Spacecraft", *Deep Space Network Space Programs Summary 37-39*, Vol. III, pp. 18-23, Jet Propulsion Laboratory, Pasadena California, May 31, 1966.
13. Campbell, J.K., Synnott, S.P., "Gravity Field of the Jovian System from Pioneer and Voyager Tracking Data," *The Astronomical Journal*, Vol. 90, No. 2, pp. 364-372, February 1985.
14. Schubert, G. *et al*, "Gravitational Coefficients and Internal Structures of the Icy Galilean Satellites: An Assessment of Galileo Orbiter Mission", *Icarus*, No. 111, pp. 433-440, 1994.
15. Galileo Home Page on World Wide Web, <http://www.jpl.nasa.gov/galileo/index.html>.
16. Peale, S.J., Cassen, P., Reynolds, R.T., "Melting of Io by Tidal Dissipation", *Science*, No. 203, pp. 892-894, 1979.

Table A-1: Filter Parameters and 1- σ *A Priori* Uncertainties

<u>ESTIMATED</u>		<u>A Priori Uncertainty (1-sigma)</u>
State		infinite position infinite velocity
Solar Pressure	Specular Reflection	0.00245 (10% of nominal)
	Diffuse Reflection	0.0258 (10% of nominal)
OTM's		1.2% of nominal thrust. 0.1 - 0.2 degrees pointing (R.A., Dec)
Attitude turns (balanced)		2 mm/s, spherical
Attitude turns (unbalanced)		1.2% of nominal thrust. 0.1 - 0.2 degrees pointing (R.A., Dec)
RPM thruster flushes		2 - 4 mm/s along axial (spacecraft Z spin-axis) direction, 1 mm/s in orthogonal directions (spacecraft X-Y plane, lateral) (ellipsoidal)
Spin-up/down		10 mm/s axial 16 mm/s lateral (ellipsoidal)
Incoherent Doppler Bias, Drift, Drift rate		100 Hz, 0.01 Hz/s, 2.0 μ Hz/s/s
Jupiter, Earth Ephemerides		Earth-Jupiter correlated covariance given in terms of Set III parameters [Standish et al., 1995]
Jupiter	Position	1.9, 11.0, 151.3 km (radial, downtrack, normal) at G1
	Velocity	0.18, 0.026, 2.0 mm/s (radial, downtrack, normal) at G1
	GM	100 km ³ /s ²
	J ₂	1.0x10 ⁻⁶
	J ₄	5.0x10 ⁻⁶
	Pole Position	0.015 deg in RA, 0.003 deg in Dec
Galilean Satellite Ephemerides		Satellite correlated covariance including masses, Jupiter Pole, mass and gravity, J ₂ , J ₄
Io	Position	6, 33, 25 km (radial, downtrack, normal)
	Velocity	136, 26, 154 cm/s (radial, downtrack, normal)
	GM	10 km ³ /s ²
Europa	Position	7, 41, 68 km (radial, downtrack, normal)
	Velocity	76, 15, 136 cm/s (radial, downtrack, normal)
	GM	10 km ³ /s ²
	J ₂	200 - 140 x10 ⁻⁶
	C ₂₂	100 - 50 x10 ⁻⁶
	S ₂₂	10 - 5 x10 ⁻⁶
Ganymede	Position	10, 41, 66 km (radial, downtrack, normal)
	Velocity	36, 10, 39 cm/s (radial, downtrack, normal)
	GM	3 km ³ /s ²
	J ₂	100 - 23 x10 ⁻⁶
	C ₂₂	20 - 5 x10 ⁻⁶
	S ₂₂	20 - 5 x10 ⁻⁶
Callisto	Position	13, 38, 29 km (radial, downtrack, normal)
	Velocity	15, 6, 9 cm/s (radial, downtrack, normal)
	GM	3 km ³ /s ²
	J ₂	30 - 10 x10 ⁻⁶
	C ₂₂	5 - 3 x10 ⁻⁶
	S ₂₂	5 - 3x10 ⁻⁶
<u>STOCHASTIC</u>		
Ionosphere zenith delay		75 cm day 15 cm night
F2 Doppler Bias		2.5 mHz
F3 Doppler Bias		2.5 mHz
Camera Pointing		0.1 deg RA, Dec (1 pixel in line and pixel) 0.30 deg Twist
<u>CONSIDERED</u>		
Station Locations 20 cm in spin radius		20 cm in z-height 2.2 μ deg in longitude Goldstone, Canberra 2.4 μ deg in longitude Madrid
Troposphere zenith delay		4.0 cm wet 1.0 cm dry
Optical center finding in line and pixel		0.25% of satellite diameter
Earth	Position	0.007, 1.0, 1.7 km (radial, downtrack, normal)
	Velocity	0.2, 0.002, 0.3 mm/s (radial, downtrack, normal)

Table A-2: Selected Orbit Determination Data Spans

ID	Radiometric Span	OPNAV Span	Days	I	E	G	C	Supporting Activity
Ganymede-1 Approach								
OD110	96/01/02 17:36 - 96/03/20 15:58	-	77.9	0	0	0	0	OD Update
OD113	01/18 09:46 - 04/16 17:50	-	89.3	0	0	0	0	OTM-4 Design
OD115	95/12/08 22:45 - 06/03 11:09	06/03 17:05 - 06/03 17:41	179.5	0	0	2	0	OTM-5 Design
OD117	95/12/08 22:45 - 06/16 09:35	06/03 17:05 - 06/16 09:15	190.4	0	0	15	0	OTM-6 Nominal Design
OD118	95/12/08 22:45 - 06/23 17:28	06/03 17:05 - 06/23 06:55	197.8	0	0	25	0	OTM-6 Tweak Design
Ganymede-2 Approach								
OD123	06/18 00:01 - 06/27 16:58	06/17 17:27 - 06/23 06:55	9.7	0	0	10	0	OTM-7 Design/DSS-63 Predicts
OD124	06/01 01:47 - 06/28 07:09	06/03 17:05 - 06/23 06:55	27.2	0	0	25	0	G2 Reference Traj Update
OD128	06/18 00:01 - 07/26 06:58	06/17 17:27 - 06/23 06:55	38.3	0	0	10	0	OTM-8 Design
OD130	06/27 12:44 - 08/19 07:50	08/10 01:58 - 08/10 02:34	52.8	0	0	2	0	OTM-9 Design
OD131	06/27 12:44 - 08/28 14:58	08/10 01:58 - 08/24 10:08	62.1	0	0	7	0	OTM-10 Nominal Design
OD132	06/27 12:44 - 09/03 13:28	08/10 01:58 - 09/02 09:44	68.0	0	2	9	0	OTM-10 Tweak Design (Cancelled)
Callisto-3 Approach								
OD135	08/21 02:25 - 09/07 06:58	08/21 12:22 - 09/02 09:44	17.2	0	2	7	0	OTM-11 Design.
OD137	09/01 12:38 - 09/27 21:17	-	26.4	0	0	0	0	OTM-12 Design
OD138	09/01 12:38 - 10/23 07:43	09/01 21:43 - 10/23 05:58	51.8	0	4	5	3	OTM-13 Nominal Design
OD139	09/01 12:38 - 10/31 03:20	09/01 21:43 - 10/31 06:07	59.6	1	6	6	13	OTM-13 Tweak Design (Cancelled)
Europa-4 Approach								
OD142	10/30 15:56 - 11/05 19:06	10/30 23:32 - 10/31 00:07	6.1	0	0	0	2	OTM-14 Design
OD143	10/23 08:09 - 11/07 02:58	10/25 05:47 - 10/31 00:07	14.8	1	3	1	10	Post-E3A Update/E4 Reference Traj Update
OD145	10/23 08:09 - 11/18 18:27	10/25 05:47 - 10/31 00:07	26.4	1	2	1	10	OTM-15 Design
OD146	10/23 08:09 - 12/09 17:56	10/25 05:47 - 12/07 16:45	47.4	3	7	5	11	OTM-16 Nominal Design
OD148	10/23 08:09 - 12/14 13:58	10/25 05:47 - 12/14 08:54	52.2	4	13	10	14	OTM-16 Tweak Design
Europa-6 Approach								
OD151	12/02 20:40 - 12/20 02:57	12/02 20:00 - 12/14 17:30	17.3	3	11	9	5	OTM-17 Design
OD153	12/02 20:40 - 12/29 16:31	12/02 20:00 - 12/14 17:30	26.8	3	11	9	5	OTM-18 Design
OD154	12/02 20:40 - 97/01/05 17:41	12/02 20:00 - 12/14 17:30	33.9	3	11	9	5	E6 Reference Traj Update
OD155	12/02 20:40 - 02/03 13:14	12/02 20:00 - 12/14 17:30	62.7	3	11	9	5	OTM-19 Design
OD156	12/02 20:40 - 02/16 13:31	12/02 20:00 - 97/02/16 06:18	75.7	4	12	15	5	OTM-20 Design (Cancelled)
Ganymede-7 Approach								
OD159	97/02/07 17:10 - 02/21 03:48	02/09 01:09 - 02/16 06:18	13.4	1	1	6	0	OTM-21 Design
OD161	02/07 17:10 - 02/22 14:03	02/09 01:09 - 02/16 06:18	14.9	1	1	6	0	G7 Reference Traj Update
OD163	02/07 17:10 - 03/04 21:58	02/09 01:09 - 02/16 06:18	25.2	1	1	6	0	OTM-22 Design
OD165	02/07 17:10 - 03/30 05:49	02/09 01:09 - 03/30 02:12	50.5	3	1	14	0	OTM-23 Design
Ganymede-8 Approach								
OD167	03/17 10:49 - 04/05 18:58	03/28 15:07 - 03/30 02:12	19.3	2	0	8	0	OTM-24 Design
OD168	03/17 10:49 - 04/07 15:58	03/28 15:07 - 03/30 02:12	21.2	2	0	8	0	G8 Reference Traj Update
OD169	03/17 10:49 - 04/14 12:20	03/28 15:07 - 03/30 02:12	28.1	2	0	8	0	OTM-25 Design.
OD170	03/17 10:49 - 05/02 14:58	03/28 15:07 - 03/30 02:12	46.2	2	0	8	0	OTM-26 Design (Cancelled)
Callisto-9 Approach								
OD172	04/24 05:43 - 05/07 20:58	-	13.6	0	0	0	0	OTM-27 Design
OD173	04/24 05:43 - 05/12 09:45	-	18.2	0	0	0	0	C9 Reference Traj Update
OD174	04/24 05:43 - 05/19 18:47	-	25.5	0	0	0	0	Jupiter Occultation prediction
OD175	04/24 05:43 - 05/26 18:21	-	32.5	0	0	0	0	OTM-28 Design
OD177	04/24 05:43 - 06/18 16:46	-	55.5	0	0	0	0	OTM-29 Design (Cancelled)
Callisto-10 Approach								
OD181	06/03 10:02 - 07/07 15:20	-	34.2	0	0	0	0	OTM-30 design
OD182	06/03 10:02 - 07/16 06:30	-	42.9	0	0	0	0	Post-C9 occultation prediction
OD183	06/03 10:02 - 07/28 13:45	07/27 14:02 - 07/27 14:11	55.1	0	0	0	0	OTM-31 design
OD184	06/03 10:02 - 08/26 03:28	07/27 14:02 - 08/03 21:25	83.7	8	0	0	0	OTM-31design
OD185	06/03 10:02 - 09/10 21:28	07/27 14:02 - 08/03 21:25	99.5	8	0	0	0	OTM-32 design
Europa-11 Approach								
OD186	08/22 21:34 - 09/17 02:58	-	25.2	0	0	0	0	OTM-33 design
OD188	08/22 21:34 - 10/13 08:16	-	51.5	0	0	0	0	OTM-34 design
OD189	08/22 21:34 - 10/24 23:39	-	63.1	0	0	0	0	OTM-35 design
Europa-12 Approach								
OD192	10/21 17:14 - 11/07 03:30	-	16.4	0	0	0	0	OTM-36 design
OD193	10/21 17:14 - 11/13 19:32	-	23.1	0	0	0	0	Occultation predictions
OD194	10/21 17:14 - 11/19 18:58	-	29.1	0	0	0	0	OTM37 design
OD195	10/21 17:14 - 12/09 19:19	-	49.1	0	0	0	0	OTM-38 design
OD197	11/27 15:34 - 12/16 18:58	-	19.1	0	0	0	0	OTM-39 design
OD200	11/27 15:34 - 01/14 23:49	-	48.3	0	0	0	0	OTM-40 (Europa-12 + apoiove) design.

Figure 1: Galileo Satellite Tour

3. Figure 2: Optical Navigation Opportunities at G7
Figure 2: Spacecraft Geometry at OPNAV Shuttering Times
(view from trajectory pole).

4.
Figure 3: The G1 Encounter B-Plane

5.
Figure 4: The G2 Encounter B-Plane

6.
Figure 5: The C3 Encounter B-Plane

7.
Figure 6: The E4 Encounter B-Plane

8.
Figure 7: The E6 Encounter B-Plane

9.
Figure 8: The G7 Encounter B-Plane

10.
Figure 9: The G8 Encounter B-Plane

11.
Figure 10: The C9 Encounter B-Plane

12.
Figure 11: The C10 Encounter B-Plane

13.
Figure 12: The E11 Encounter B-Plane

14.
Figure 13: The E12 Encounter B-Plane

15.
Fig. 14 Galileo VLBI Measurements

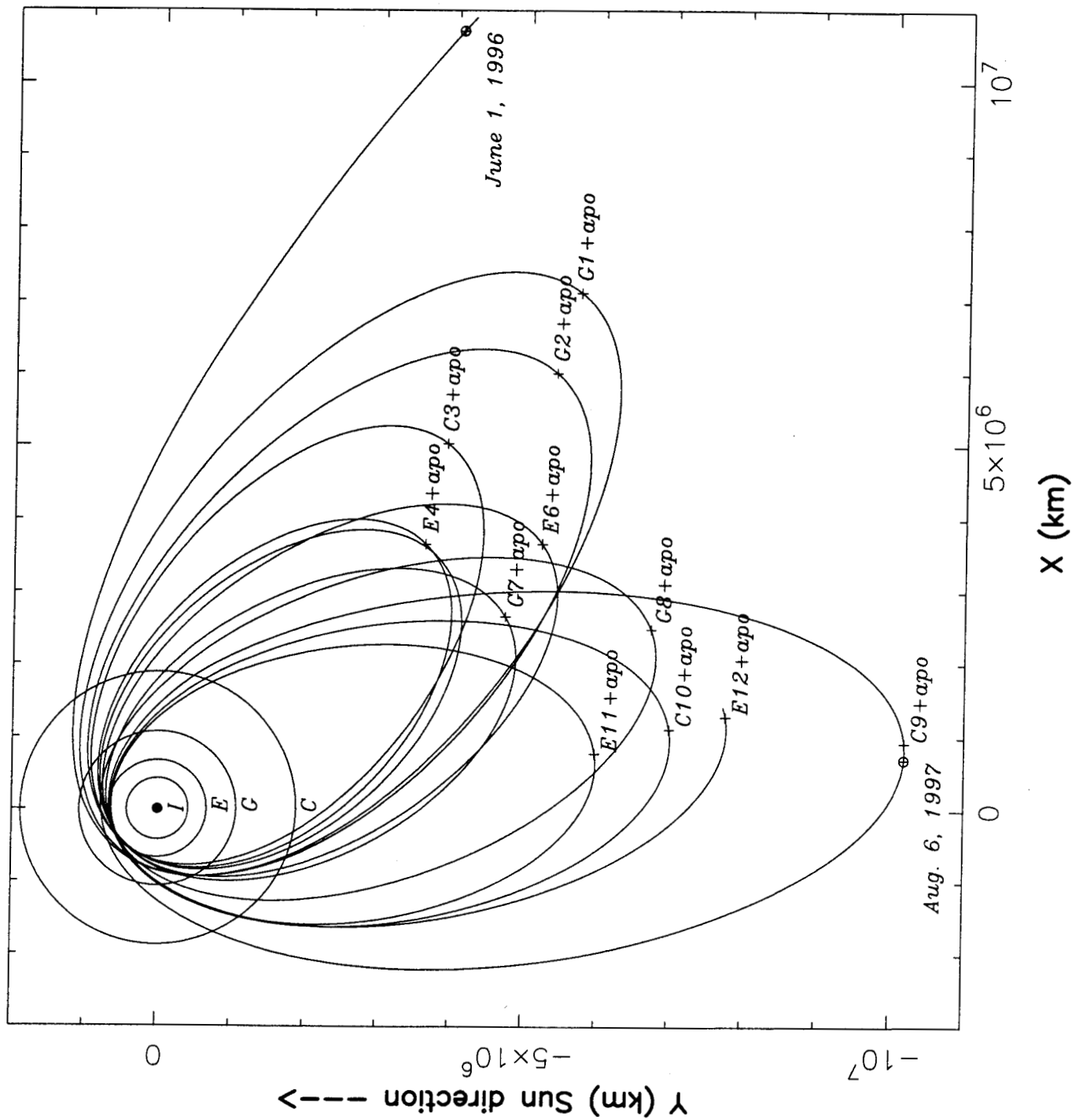
16.
Figure 15: Changes in Mass from the *A Priori*

17.
Figure 16: Improvements in 1σ Mass Uncertainties from the *A Priori*

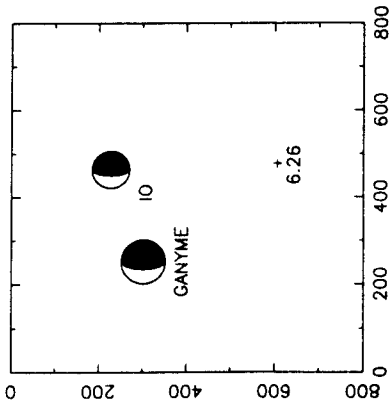
17.
Table 1: Achieved versus Predicted OD Uncertainty

Fig 1

Jovicentric Sun-fixed frame

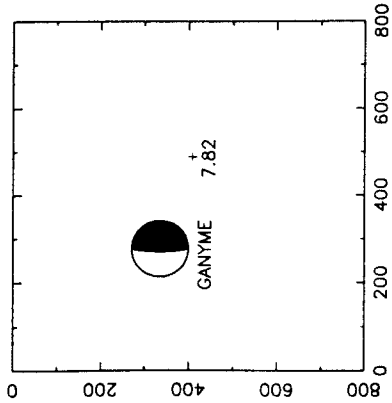


28-MAR-1997 15:07:40.500



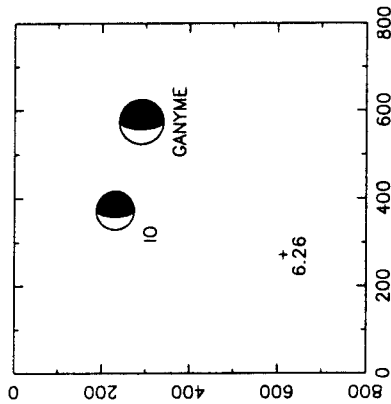
ID= 122, R= 4.139 Mkm, Cone= 55.588

29-MAR-1997 18:47:55.100



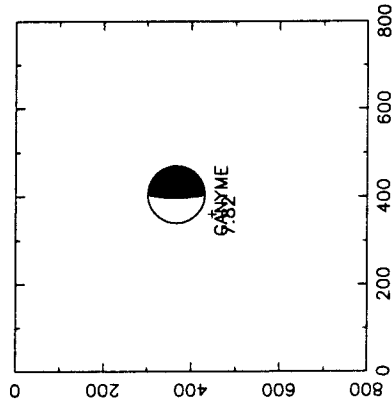
ID= 140, R= 4.029 Mkm, Cone= 67.951

28-MAR-1997 15:42:03.200



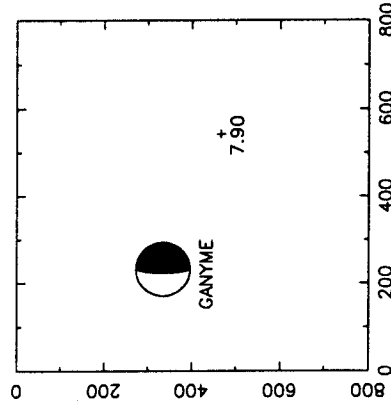
ID= 123, R= 4.096 Mkm, Cone= 55.692

29-MAR-1997 19:08:08.400



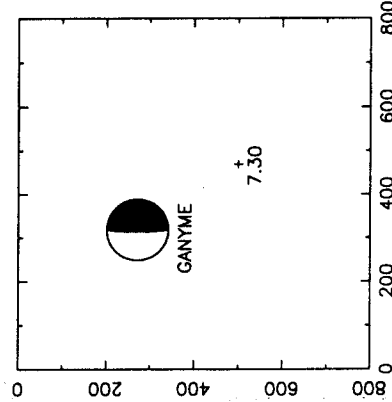
ID= 141, R= 4.012 Mkm, Cone= 68.011

29-MAR-1997 15:42:53.100



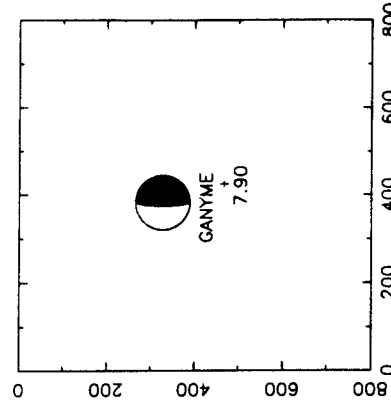
ID= 138, R= 4.177 Mkm, Cone= 66.714

30-MAR-1997 01:52:35.100



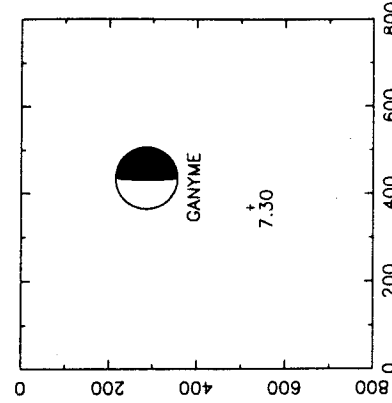
ID= 142, R= 3.673 Mkm, Cone= 70.589

29-MAR-1997 16:03:06.400



ID= 139, R= 4.161 Mkm, Cone= 66.776

30-MAR-1997 02:12:48.400



ID= 143, R= 3.656 Mkm, Cone= 70.639

Fig 3

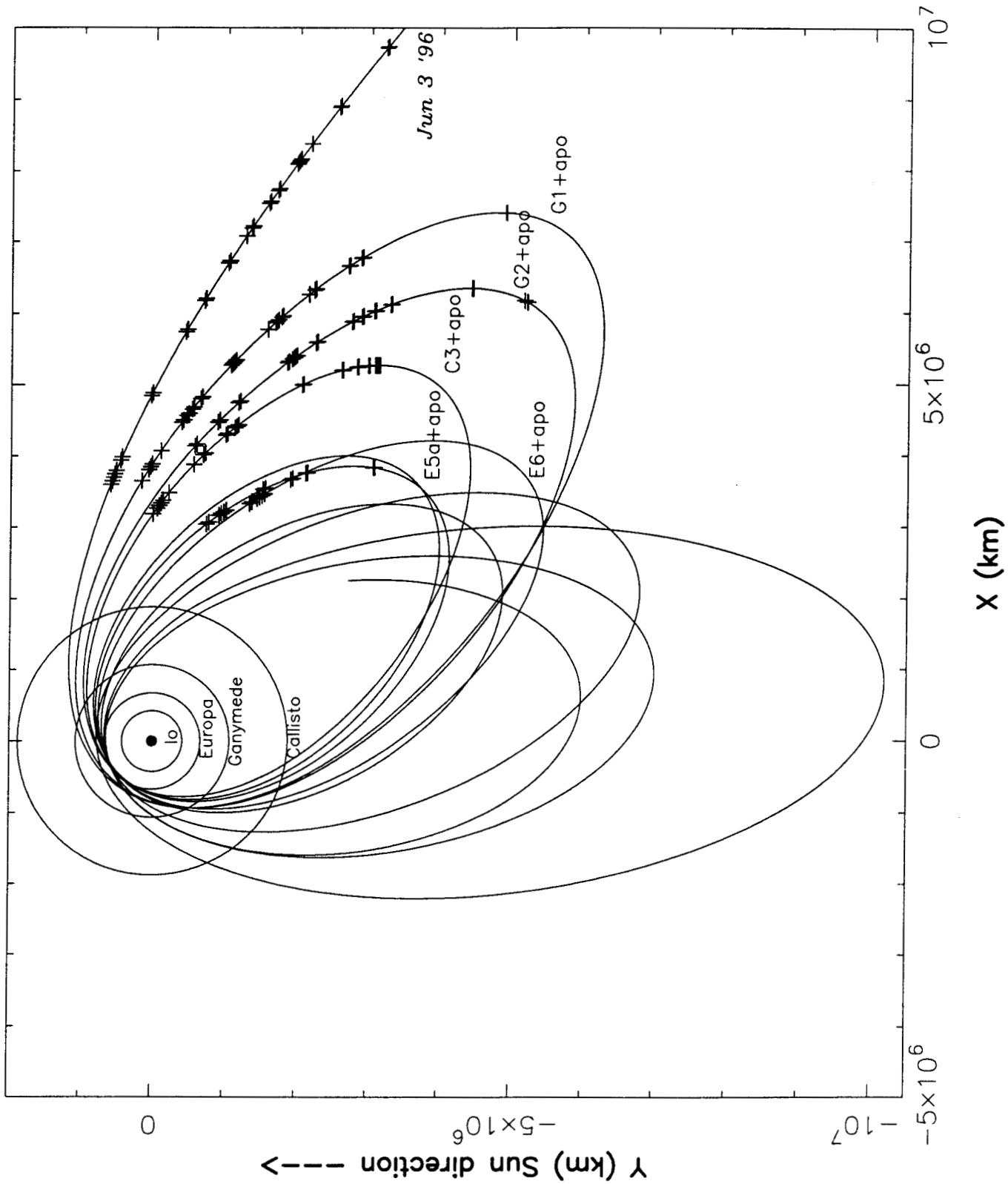


Fig B 4

Ganymede-1 B-plane (Earth-Mean-Ecliptic of 1950)

TCA = 27-JUN-1996 06:29:04.0 SCET UTC

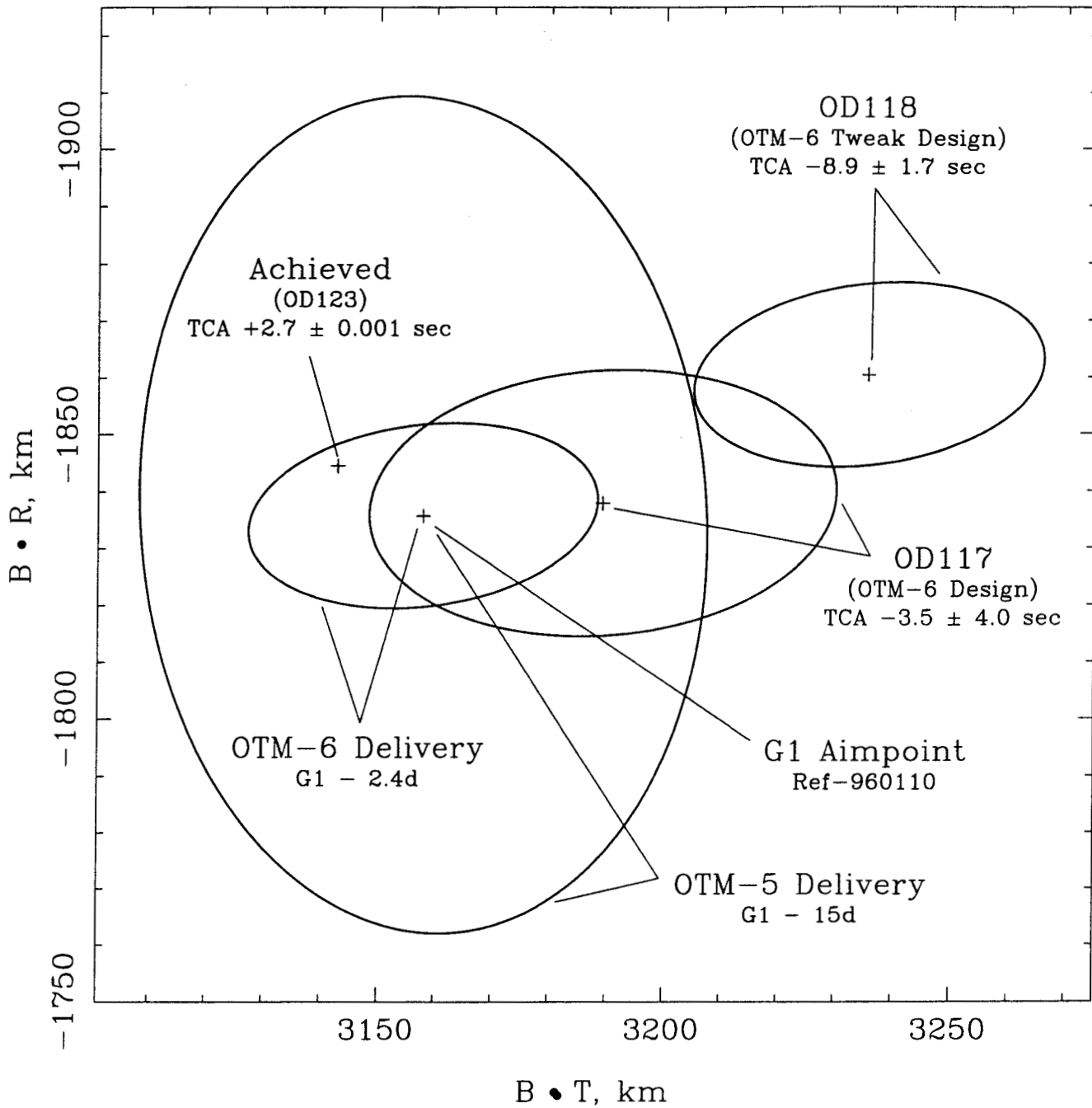


Fig 5

Ganymede-2 B-plane (Earth-Mean-Ecliptic of 1950)

TCA = 06-SEP-1996 18:59:39.0 SCET UTC

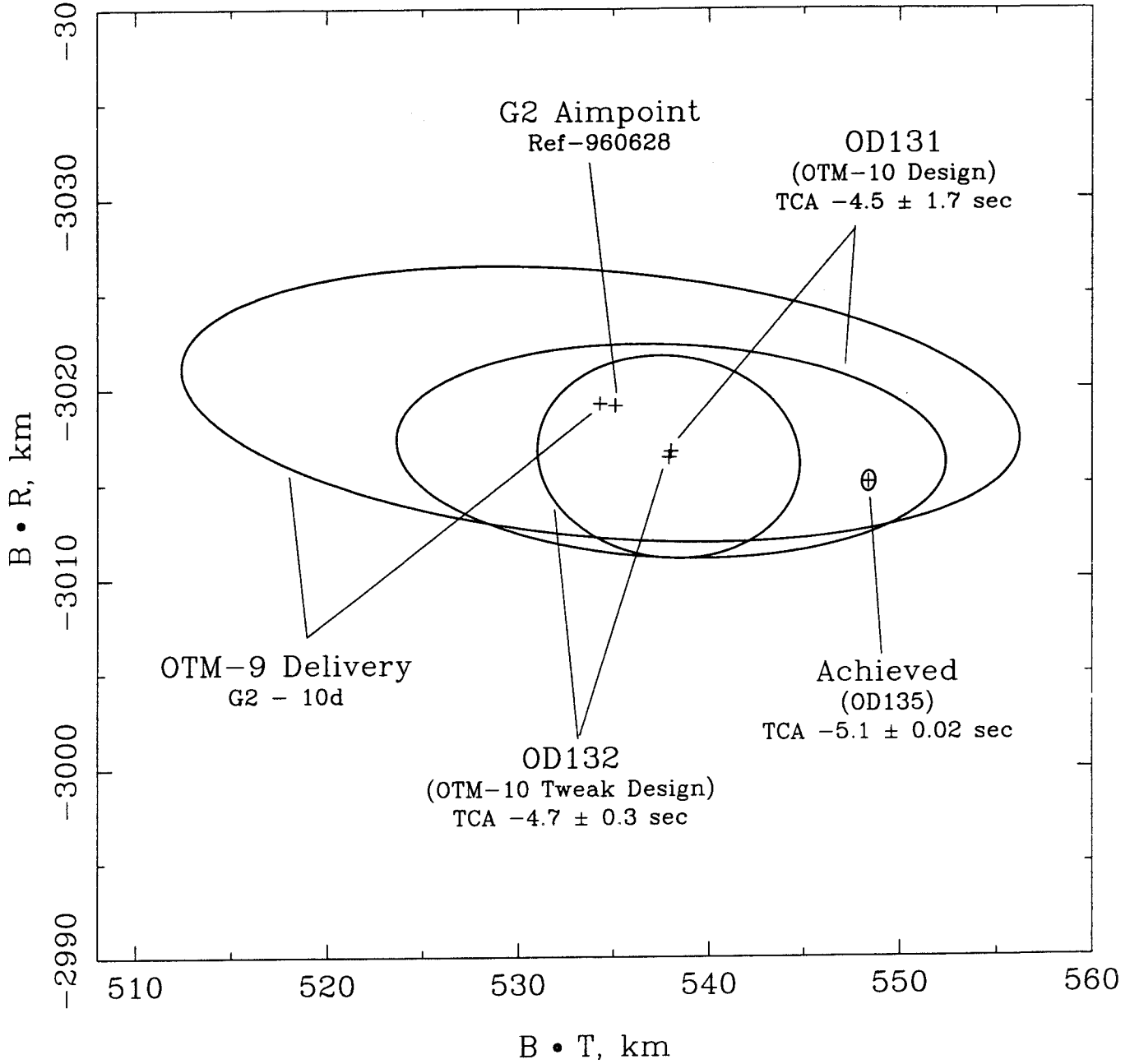


Fig 56

Callisto-3 B-plane (Earth-Mean-Ecliptic of 1950)

TCA = 04-NOV-1996 13:34:27.0 SCET UTC

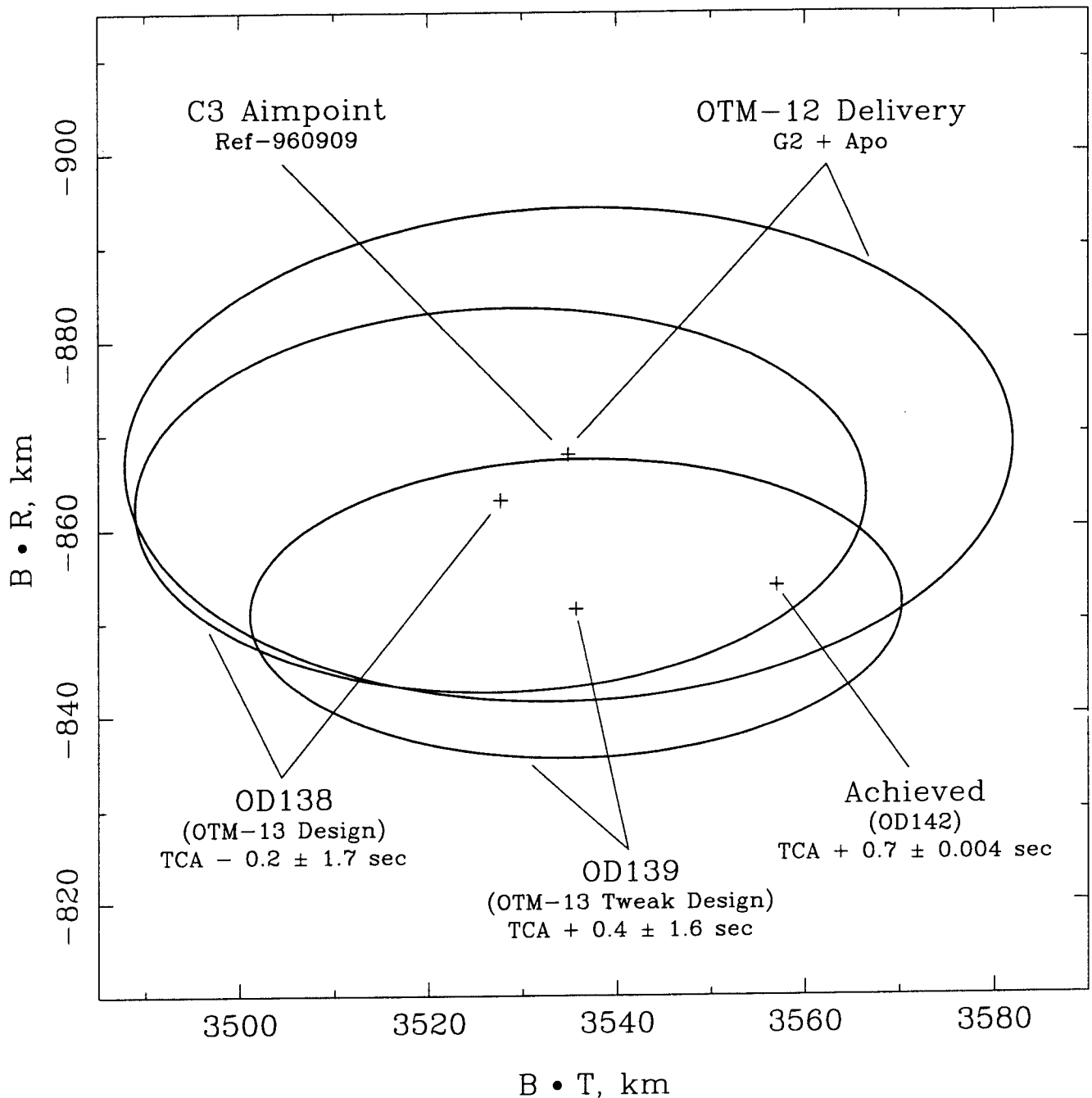


Fig 7

Europa-4 B-plane (Earth-Mean-Ecliptic of 1950)

TCA = 19-DEC-1996 06:52:56.7 SCET UTC

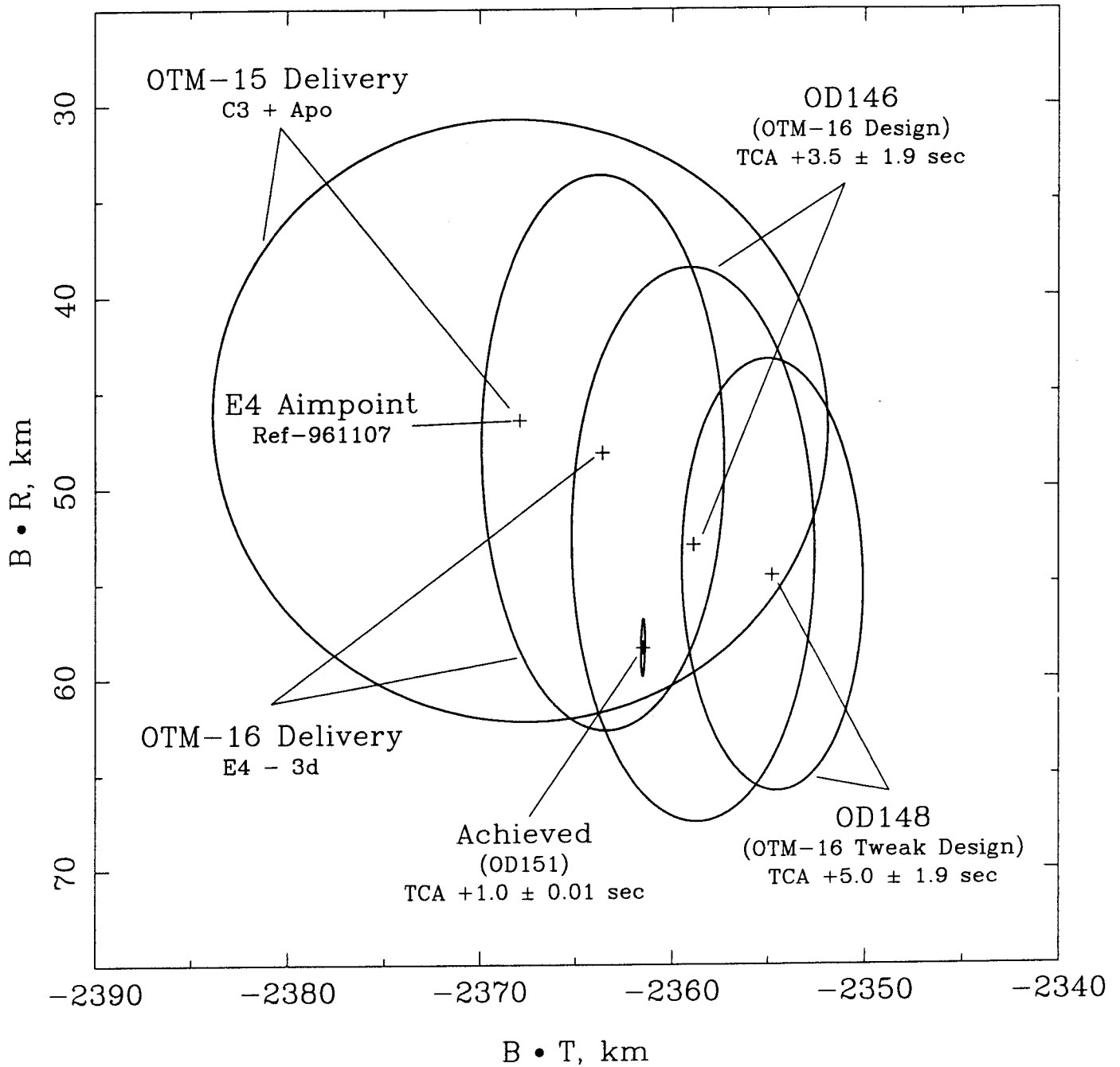


Fig 8

Europa-6 B-plane (Earth-Mean-Ecliptic of 1950)

TCA = 20-FEB-1997 17:06:13.0 SCET UTC

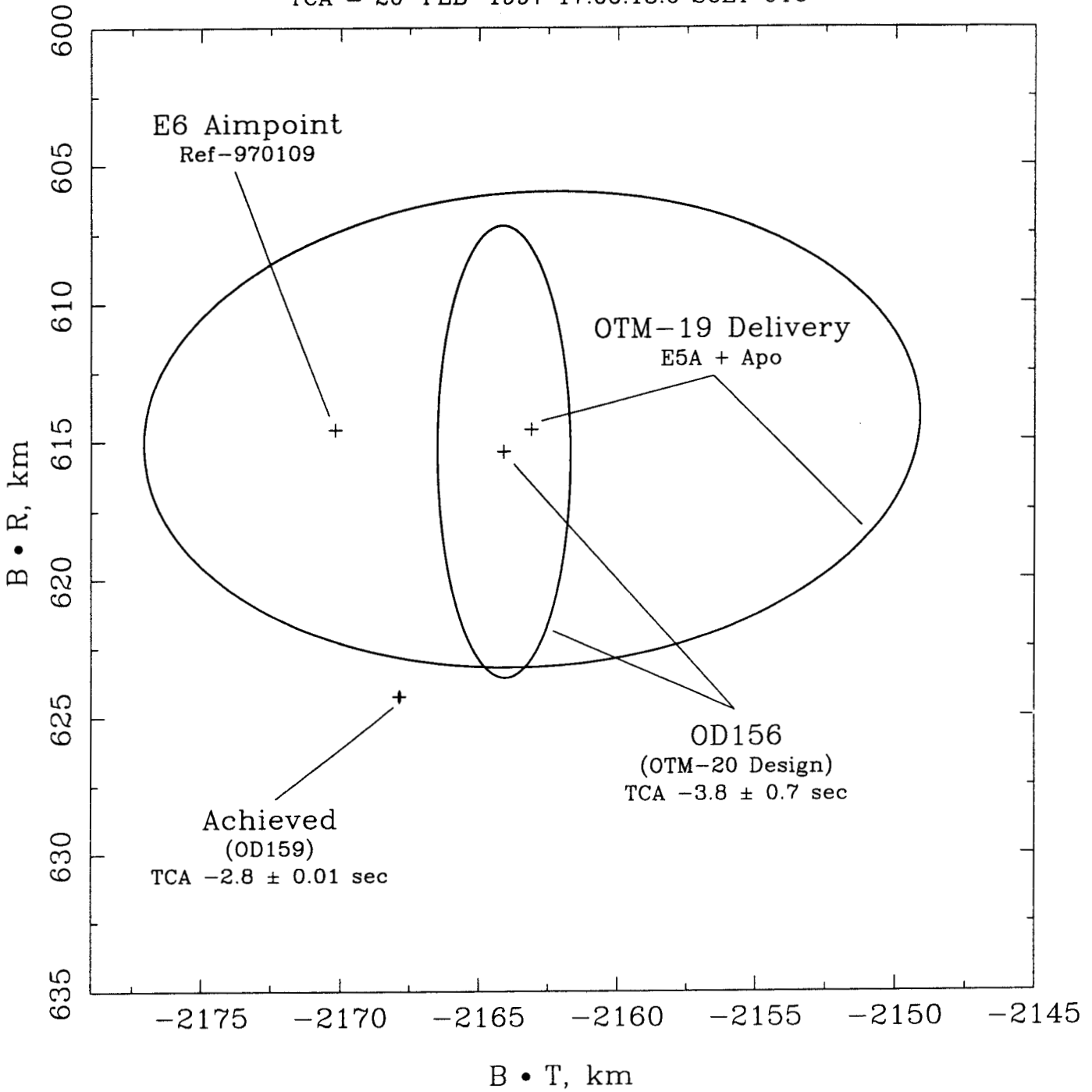
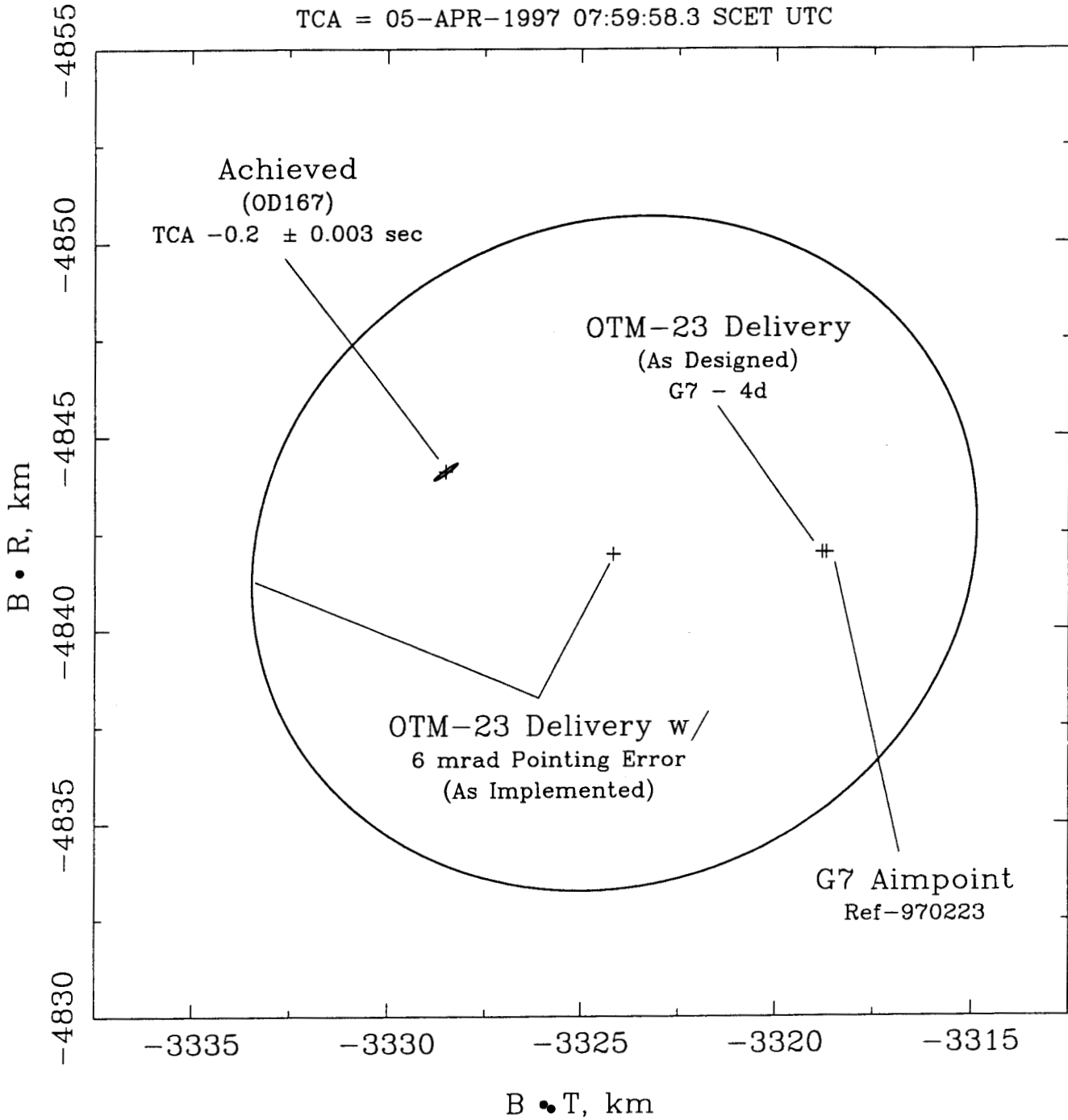


Fig 9

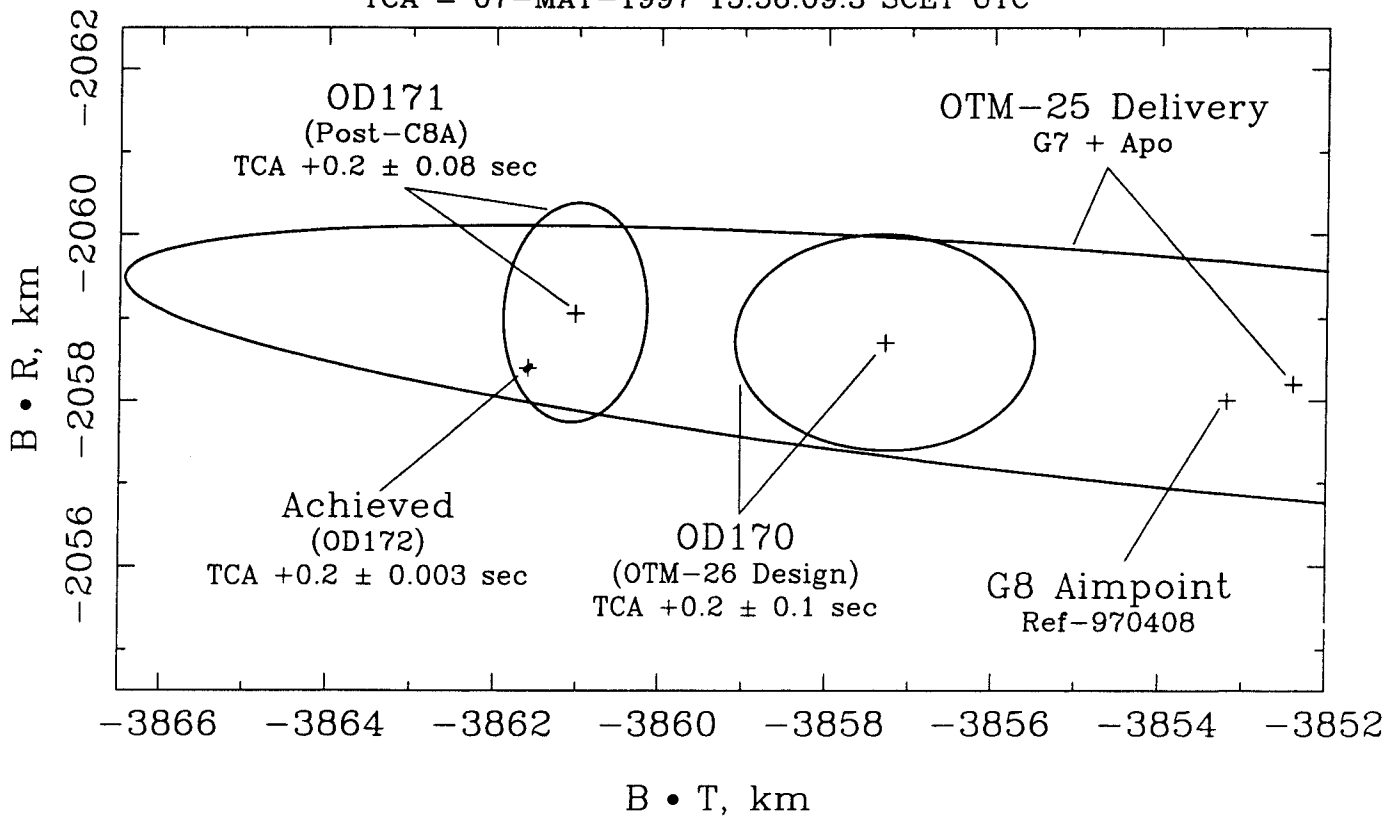
Ganymede-7 B-plane (Earth-Mean-Ecliptic of 1950)

TCA = 05-APR-1997 07:59:58.3 SCET UTC



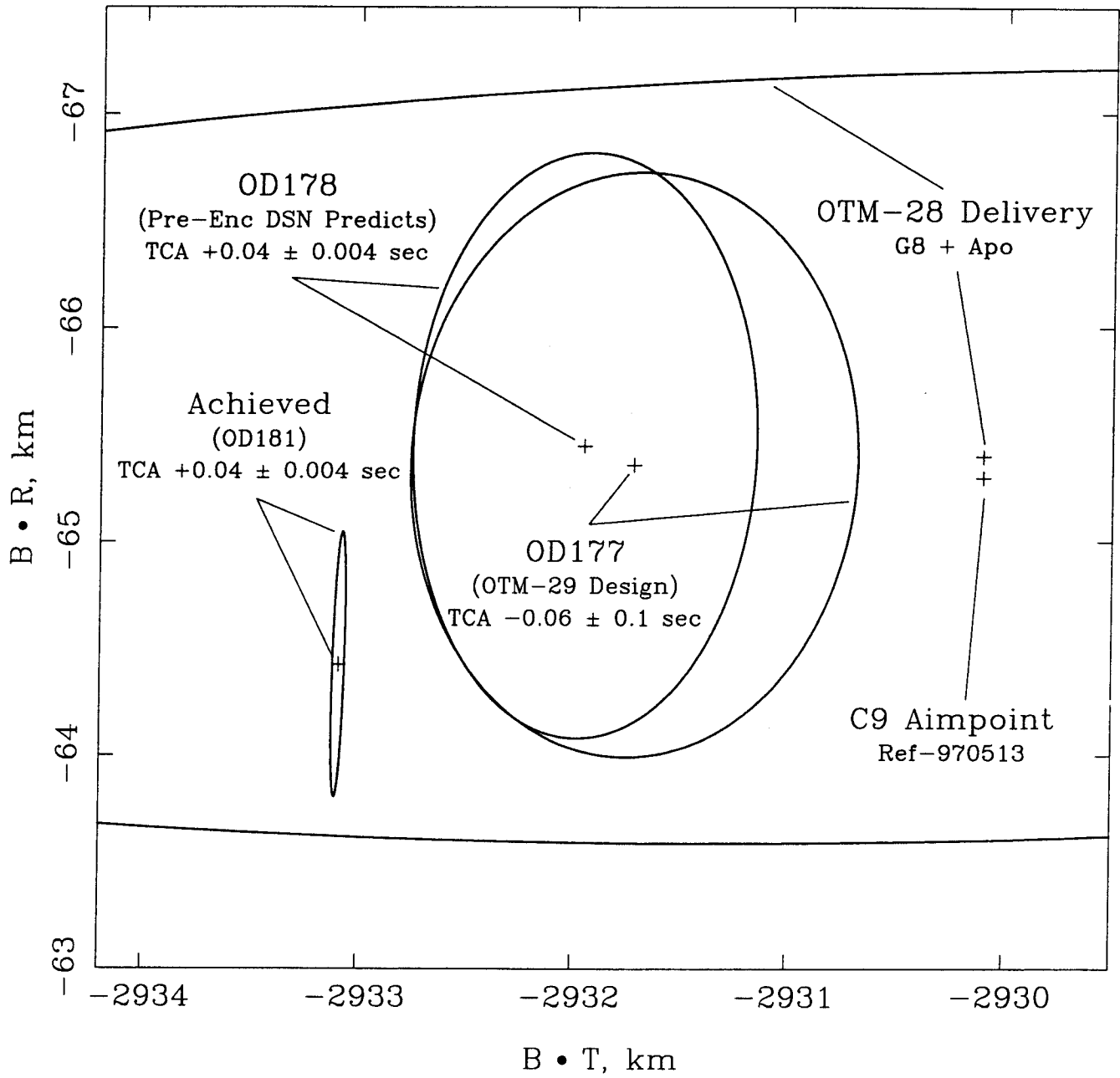
Ganymede-8 B-plane (Earth-Mean-Ecliptic of 1950)

TCA = 07-MAY-1997 15:56:09.3 SCET UTC



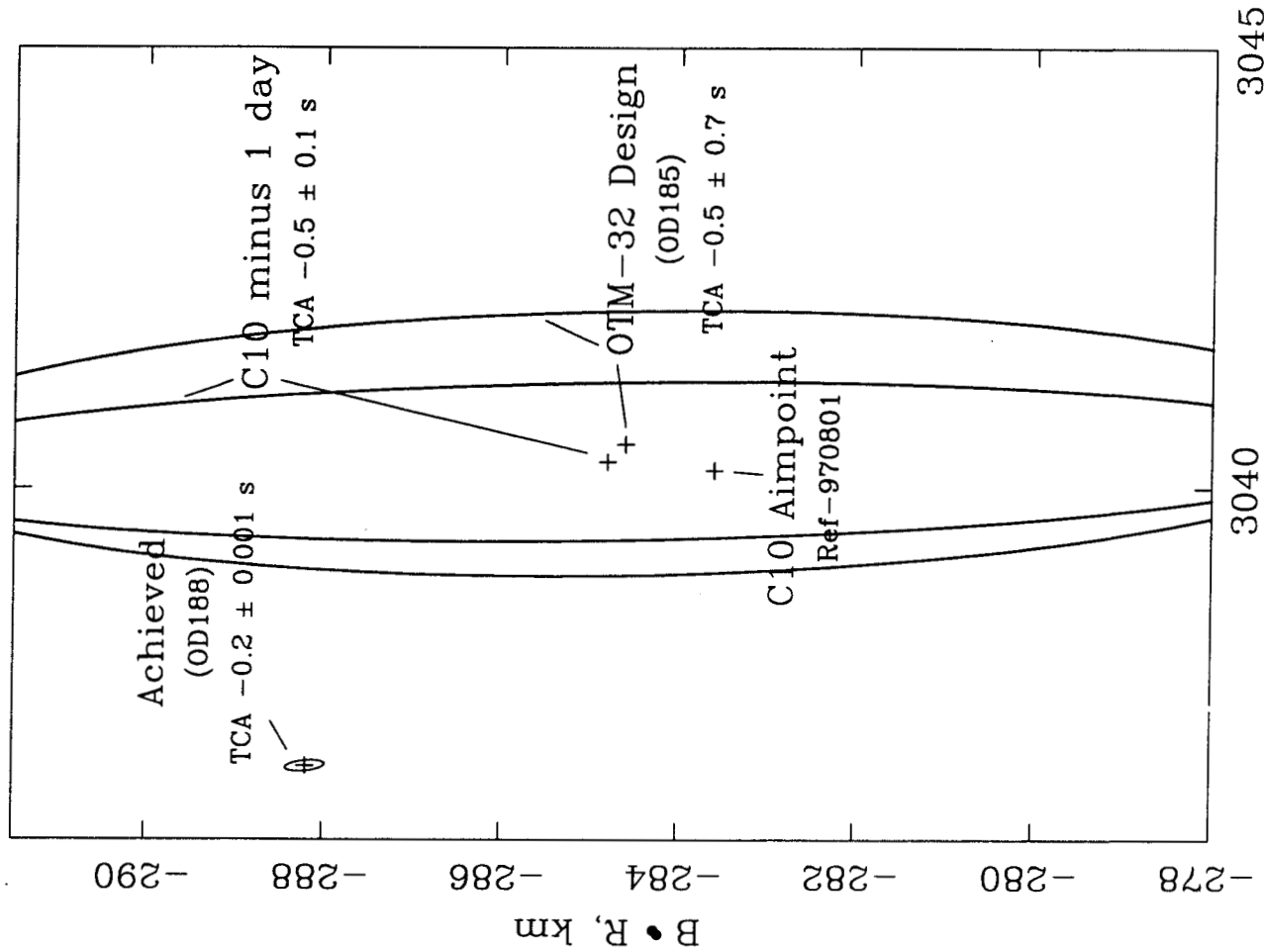
Callisto-9 B-plane (Earth-Mean-Ecliptic of 1950)

TCA = 25-JUN-1997 13:47:49.9 SCET UTC



Callisto-10 B-plane (Earth-Mean-Ecliptic of 1950)

TCA = 17-SEP-1997 00:18:54.8 SCET UTC



B • T, km

Europa-11 B-plane (Earth-Mean-Ecliptic of 1950)

TCA = 6-NOV-1997 20:31:44.2 SCET UTC

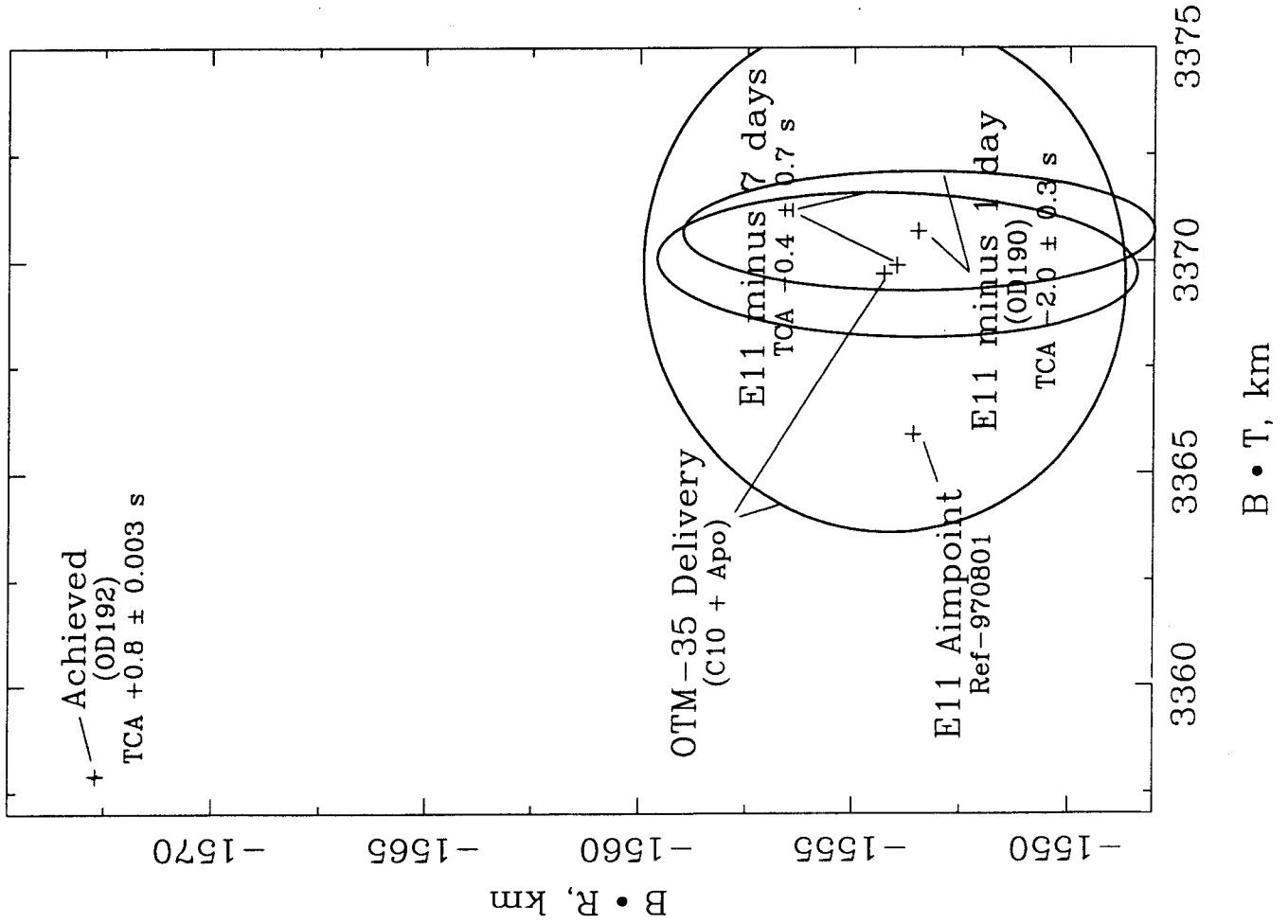
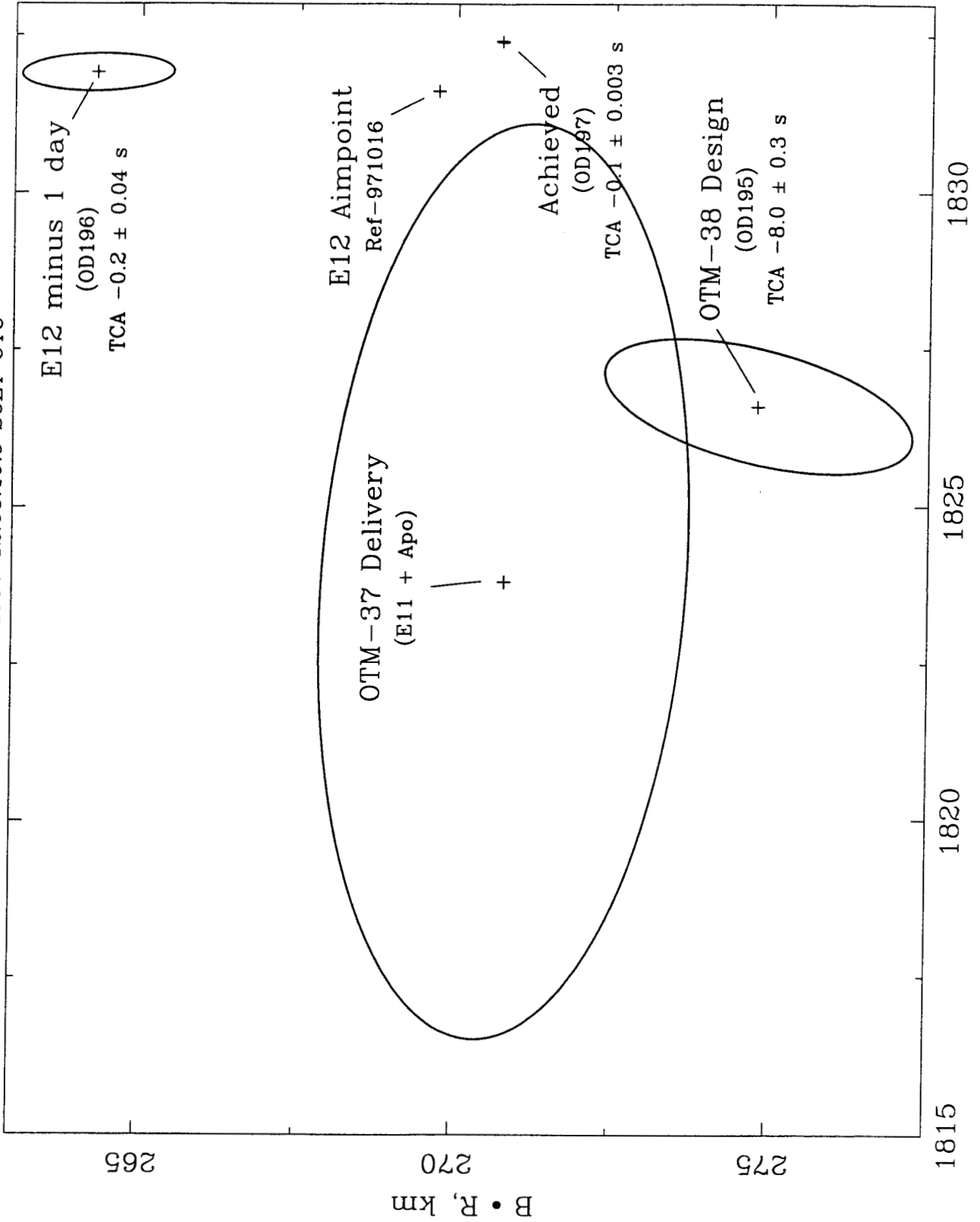


Fig 14

Europa-12 B-plane (Earth-Mean-Ecliptic of 1950)

TCA = 16-DEC-1997 12:03:19.9 SCET UTC



B • T, km

Fig 15

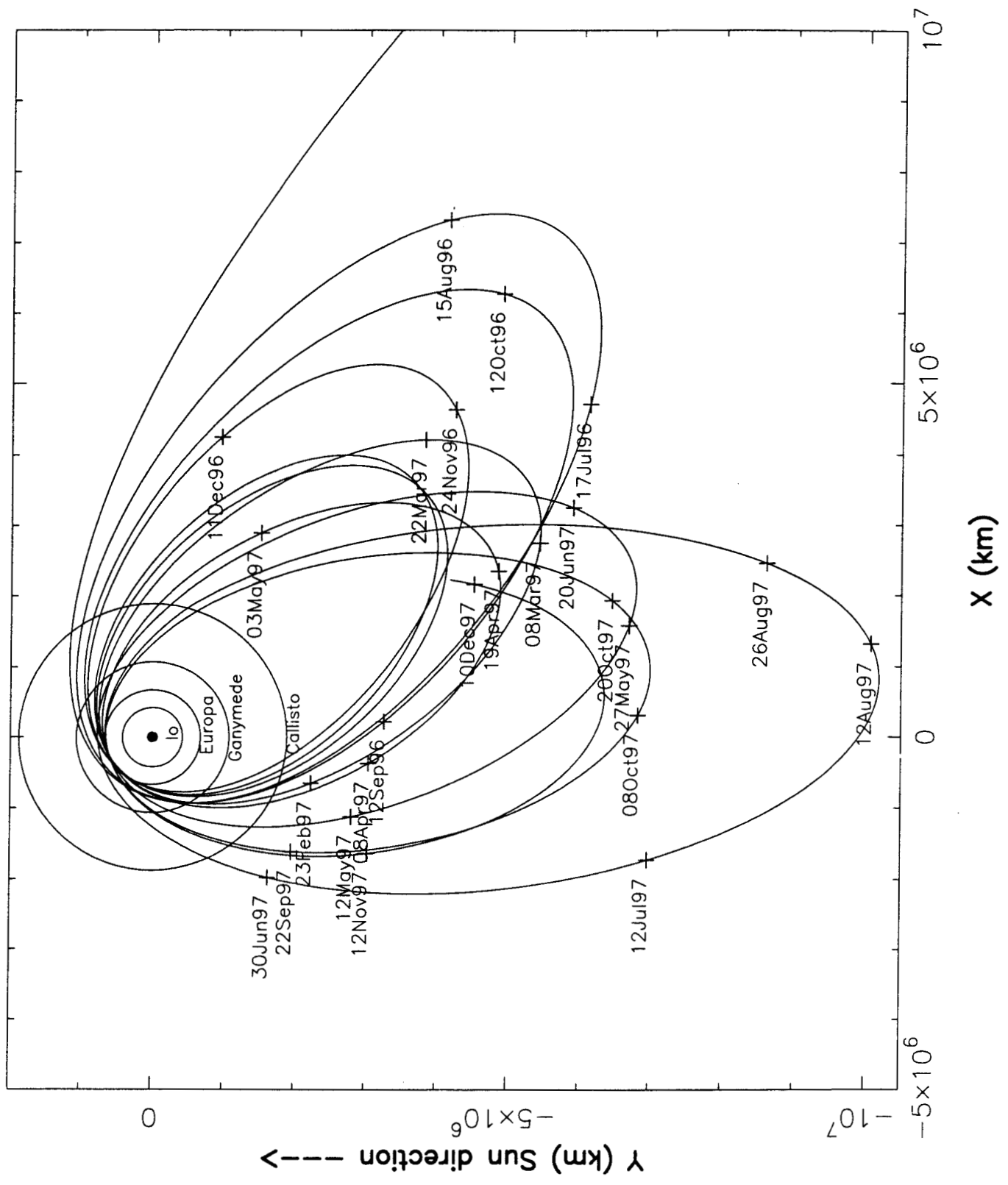


Fig 16

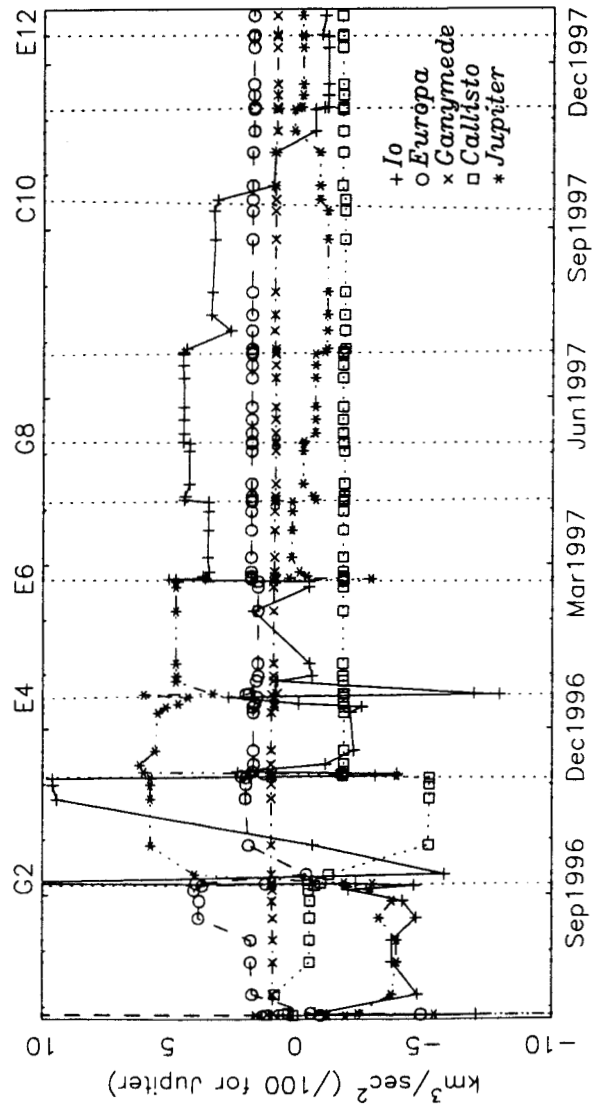


Fig 17

